Please cite this article in press as: Ichwan et al., Apple Peel and Flesh Contain Pro-neurogenic Compounds, Stem Cell Reports (2021), https://doi.org/10.1016/j.stemcr.2021.01.005

Stem Cell Reports
ISSCR
Article
OPEN ACCESS

Apple Peel and Flesh Contain Pro-neurogenic Compounds

Muhammad Ichwan,[1,2,9] Tara L. Walker,[1,2,3,9] Zeina Nicola,[1,2] Jutta Ludwig-Müller,[4] Christoph Böttcher,[5] Rupert W. Overall,[1,2] Vijay S. Adusumilli,[1,2] Merve Bulut,[1,2] Alex M. Sykes,[6] Norbert Hübner,[7] Gerardo Ramirez-Rodriguez,[8] Leonardo Ortiz-López,[8] Enrique A. Lugo-Hernández,[8] and Gerd Kempermann[1,2,*]

[1]Center for Regenerative Therapies Dresden (CRTD), Technische Universität Dresden, 01307 Dresden, Germany
[2]German Center for Neurodegenerative Diseases (DZNE) Dresden, 01307 Dresden, Germany
[3]Queensland Brain Institute (QBI), The University of Queensland, Brisbane 4072, Australia
[4]Institute for Botany, Technische Universität Dresden, 01062 Dresden, Germany
[5]Leibniz Institute of Plant Biochemistry, 06120 Halle (Saale), Germany
[6]Griffith Institute for Drug Discovery, Griffith University, Brisbane 4111, Australia
[7]Max-Delbrück-Centrum für Molekulare Medizin (MDC), 13125 Berlin, Germany
[8]Laboratory of Neurogenesis, Division of Clinical Investigations, National Institute of Psychiatry "Ramon de laFuente Muñiz," Mexico DF, Mexico
[9]These authors contributed equally
*Correspondence: gerd.kempermann@dzne.de
https://doi.org/10.1016/j.stemcr.2021.01.005

SUMMARY

As mammals evolved with exposure to particular diets, naturally abundant compounds may have become part of the set of environmental co-determinants that shaped brain structure and function. Here we investigated whether bioactive factors found in apples directly affect hippocampal neurogenesis in the adult mouse. We found that quercetin, the most abundant flavanol in apple peel, was anti-proliferative at high concentrations but pro-neurogenic at low concentrations. This was confirmed *in vivo*, with intraperitoneally delivered quercetin promoting survival and neuronal differentiation, without affecting proliferation. Using a bioassay-guided fractionation approach we also identified additional pro-neurogenic compounds in apple flesh that were not related to flavonoids. We found that 3,5-dihydroxybenzoic acid significantly increased neural precursor cell proliferation and neurogenesis. This work shows that both flavonoids and 3,5-dihydroxybenzoic acid are pro-neurogenic, not only by activating precursor cell proliferation but also by promoting cell-cycle exit, cellular survival, and neuronal differentiation.

INTRODUCTION

"An apple a day keeps the doctor away." There may be some truth to this aphorism. Apart from being a source of energy, food is known to influence an individual's overall fitness. A growing number of studies have demonstrated the health benefits of phytochemicals, the chemical substances found in plants (for review see Dillard and German, 2000). Active dietary compounds are also vital for maintaining cognitive function. One of the processes underlying this maintenance is brain plasticity, whereby structural and functional modifications occur in response to internal and external stimuli. Adult hippocampal neurogenesis is a particular form of brain plasticity in which functional neurons are generated throughout life and integrated into the existing circuitry, thereby mediating particular forms of learning and memory.

Flavonoids, the abundant phytonutrients found in fruits and vegetables, can modulate molecular signaling pathways that influence these cognitive processes (Spencer, 2009). Prominent examples of flavonoids and polyphenols are resveratrol (found in the skin of red grapes and in red wine) and epigallocatechin-3-gallate (EGCG; found in green tea). In the case of resveratrol, the biological activity has been traced to the intracellular regulation of Sirt1 and other sirtuins (Prozorovski et al., 2008). We and others have shown that both EGCG and resveratrol affect adult hippocampal neurogenesis (Ortiz-Lopez et al., 2016; Torres-Perez et al., 2015; Yoo et al., 2010). However, although some positive indications have been reported, intervention trials based on the consumption of resveratrol and similar factors have often proved disappointing (van der Made et al., 2015). One reason, other than questions of bioavailability, might be that plants actually contain a very large number of potentially active compounds. Georgiev et al. (2014), for example, list 20 flavonoids from grapes alone, which likely work in concert to produce beneficial effects on central nervous system function, including positive effects on learning and memory.

As apples are one of the most widely consumed fruits worldwide, resulting in a generalized exposure across cultures, we investigated whether they contain substances that sustain or promote adult hippocampal neurogenesis. We took a two-pronged approach, first studying quercetin, the most abundant flavonoid in apple peel (Bhagwat and Haytowitz, 2016), and second extending our investigation to identify additional pro-neurogenic factors in the fruit.

This is an open access article under the CC BY-NC-ND license (http://creativecommons.org/licenses/by-nc-nd/4.0/).

RESULTS

Quercetin Promotes Cell-Cycle Exit and Neuronal Differentiation *In Vitro*

Quercetin has been linked to several neuroprotective mechanisms, particularly in relation to microglial function (Nichols et al., 2015). This class of phytochemicals can also exert antioxidant effects due to its capacity to scavenge reactive oxygen species. Although quercetin and other natural compounds could affect adult neurogenesis through more than one pathway, we focused on their effect on stem cells, from which the adult-born neurons in the hippocampus originate. We first used the monolayer culture system, which consists of a relatively pure population of putative stem and progenitor cells, to establish a dose-response curve. In line with reports of inhibitory effects of high doses of quercetin on cancer stem cells, we found that incorporation of the thymidine analog 5-bromo-2′-deoxyuridine (BrdU), as a measure of proliferative activity, was reduced at concentrations of 25 μM and higher (Figures 1A and 1B). At concentrations up to 35 μM, this was not due to increased cytotoxicity, which was, however, detected at even higher doses with the lactate dehydrogenase assay (Figure 1C) and 7-AAD staining (Figure 1D). Cell-cycle analysis based on propidium iodide incorporation and flow cytometric analysis revealed that 25 μM quercetin reduced S-phase entry (Figure 1E) and caused the cells to accumulate in the G1 phase (Figure 1E). Western blot analysis for cell-cycle-related proteins showed that CDK4 levels were significantly decreased when 25 μM quercetin was added to cells grown under proliferation conditions (Figure 1F). In contrast, no change in the expression of either cyclin D1 or p27 was observed following the addition of 25 μM quercetin to the proliferating cells (Figure 1F).

The above data indicate that quercetin upregulates the cell-cycle "brake" signal to counteract the mitogenic effects of growth factors. This was further supported by our observation that, in the presence of growth factors, 25 μM quercetin increased the number of cells with neuron-like morphology (Figures 1G and 1H) and βIII-tubulin expression (an immature neuronal marker; Figures 1H and 1I), whereas expression of the stem cell marker nestin was decreased (Figures 1H and 1J). Taken together, these findings indicate that quercetin can act pro-neurogenically even in the presence of growth factors, which normally maintain neural precursor cells (NPCs) in an undifferentiated and proliferative state *in vitro*.

Quercetin Promotes *In Vitro* Cell Survival and Stimulates Adult Neurogenesis *In Vivo*

The NPCs in monolayer cultures can be induced to differentiate into neurons or astrocytes by removal of growth factors. However, growth factor withdrawal also leads to significant cell death. As polyphenols have been shown to exert neuroprotective effects, we next examined whether quercetin supports cell survival *in vitro* during differentiation. We found that the addition of 25 μM quercetin for 4 days following growth factor withdrawal almost doubled the percentage of surviving cells (Figures 2A–2C).

Given the positive effects of quercetin *in vitro*, we next examined its effects *in vivo*. Quercetin was administered orally at 50 mg/kg, a dose previously shown to lead to sufficient accumulation of metabolites in the brain (Ishisaka et al., 2011). Proliferating cells were labeled with iododeoxyuridine (IdU) after 14 days of quercetin treatment, whereas the effect of the treatment on cell survival was assessed in a cohort of cells labeled with chlorodeoxyuridine (CldU) immediately before the treatment began (Figure 2D). After 2 weeks of quercetin treatment we observed a trend toward a decrease in proliferation (Figure 2E). In contrast, the number of $CldU^+$ cells was significantly increased (Figure 2F). Quercetin treatment resulted in a net increase in the number of newly born neurons, with a significantly higher percentage of $NeuN^+/CldU^+$ cells compared with the control group (Figures 2G and 2H), whereas the number of new astrocytes was unchanged.

Quercetin Induces Endogenous Antioxidants and the AKT Pathway

To determine how quercetin exerts an effect on cell survival, we next performed RNA microarray analysis on cells collected 24 h after growth factor withdrawal. The expression levels of 3,900 transcripts significantly changed following 25 μM quercetin treatment (Figure 3A). The top 10 positively regulated genes (Table S1) were enriched for genes related to oxidative stress (*Gsta3*, *Srxn1*, *Osgin1*), as well as Relaxin1, which has been reported to promote osteoblast differentiation (Moon et al., 2014). Remarkably, we found that *Miat*, a long non-coding RNA recently identified as a switch gene in lineage-determined neuronal progenitor cells during cortical development (Aprea et al., 2013), was among the top 10 negatively regulated transcripts. To identify putative target pathways we subjected the transcript lists to enrichment with WebGestalt and pathway analysis from the KEGG and WikiPathway databases. Following hypergeometric testing, the top 10 most significantly enriched pathways were identified (Figures 3B and 3C). These pathways were then ranked according to the ratio of genes in the sample to the overall number of members in that pathway. In both databases, pathways involved in "cell cycle," "endogenous antioxidative activity," and "cell survival" were significantly enriched, as was mitogen-activated protein kinase (MAPK) signaling. It is known that, depending on their specific chemical structure, flavonoids can either inhibit or activate these

Please cite this article in press as: Ichwan et al., Apple Peel and Flesh Contain Pro-neurogenic Compounds, Stem Cell Reports (2021), https://doi.org/10.1016/j.stemcr.2021.01.005

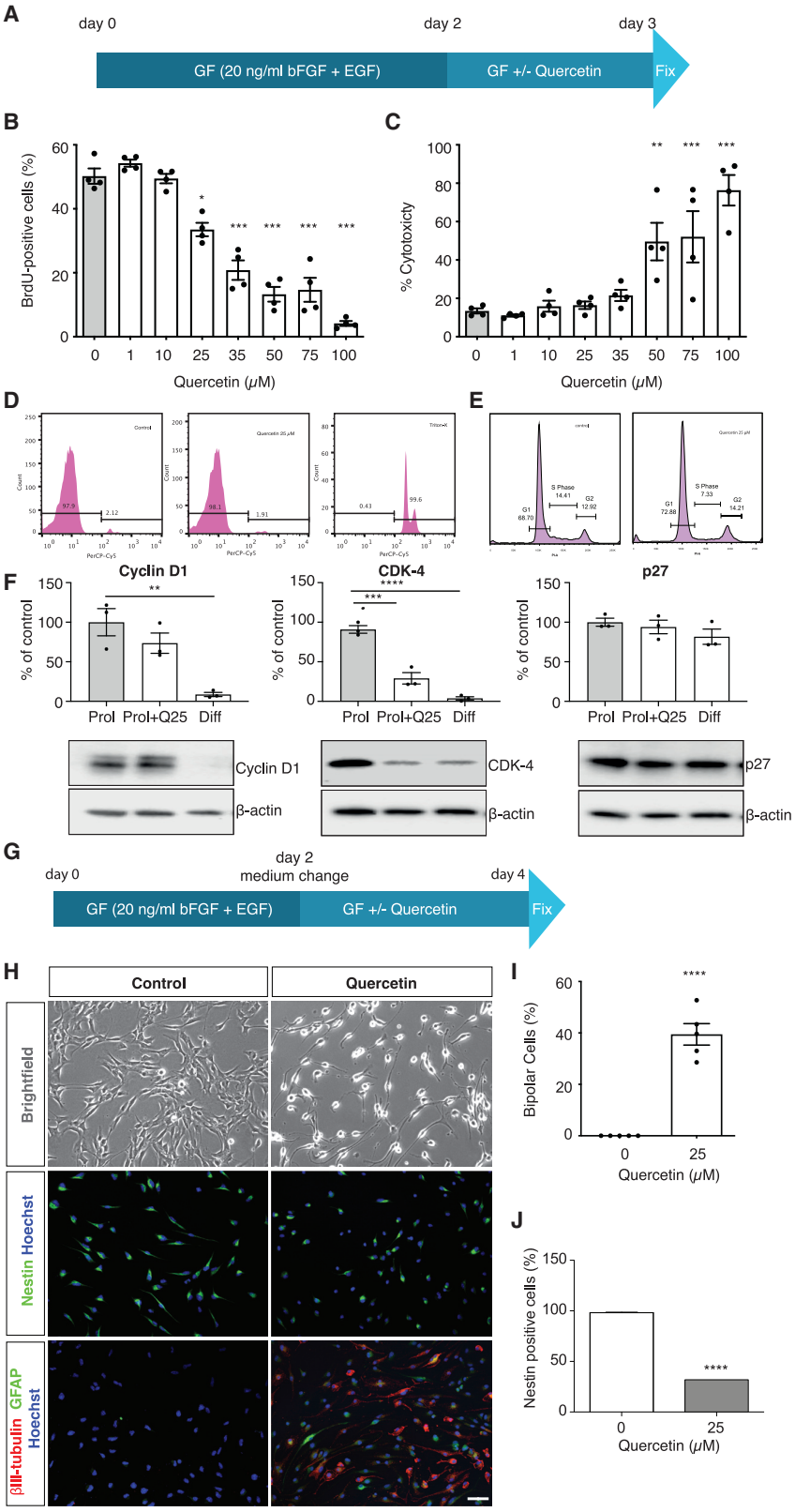

Figure 1. Quercetin Inhibits the Cell Cycle and Induces NPC Differentiation

(A) Schematic of the monolayer NPC culture with 24 h quercetin treatment.

(B and C) (B) Quercetin decreased BrdU-labeled cells dose dependently. (C) Quercetin concentrations of ≥50 μM significantly increased the number of dead cells. n = 4 independent experiments in (B) and (C).

(D) Cell-cycle analysis using propidium iodide staining revealed a decreased number of cells entering S phase after 24 h of 25 μM quercetin treatment.

(E) 7-AAD staining confirmed that quercetin (25 μM) does not induce cell death.

(F and G) (F) Western blot analysis revealed that quercetin treatment of proliferating precursor cells resulted in the downregulation of CDK4 and no change in the expression levels of cyclin D2 or p27. Cells cultured for 24 h without growth factors (Diff) were used as a control for cell-cycle arrest. n = 3 independent experiments. (G) Experimental scheme.

(H) NPCs develop "neuron-like" bipolar characteristics (top row). In addition, they downregulate nestin expression (middle) and upregulate expression of the neuronal marker βIII-tubulin (bottom). Scale bar, 50 μm.

(I and J) (I) Quercetin (25 μM) significantly increased the percentage of cells with a bipolar morphology. n = 5 independent experiments. (J) Quercetin (25 μM) significantly decreased the percentage of nestin$^+$ cells.

One-way ANOVA with Dunnett's post hoc test in (B) and (C) and Student's t test in (I) and (J). GF, growth factors. *$p < 0.05$, **$p < 0.01$, ***$p < 0.001$, ****$p < 0.0001$.

Please cite this article in press as: Ichwan et al., Apple Peel and Flesh Contain Pro-neurogenic Compounds, Stem Cell Reports (2021), https://doi.org/10.1016/j.stemcr.2021.01.005

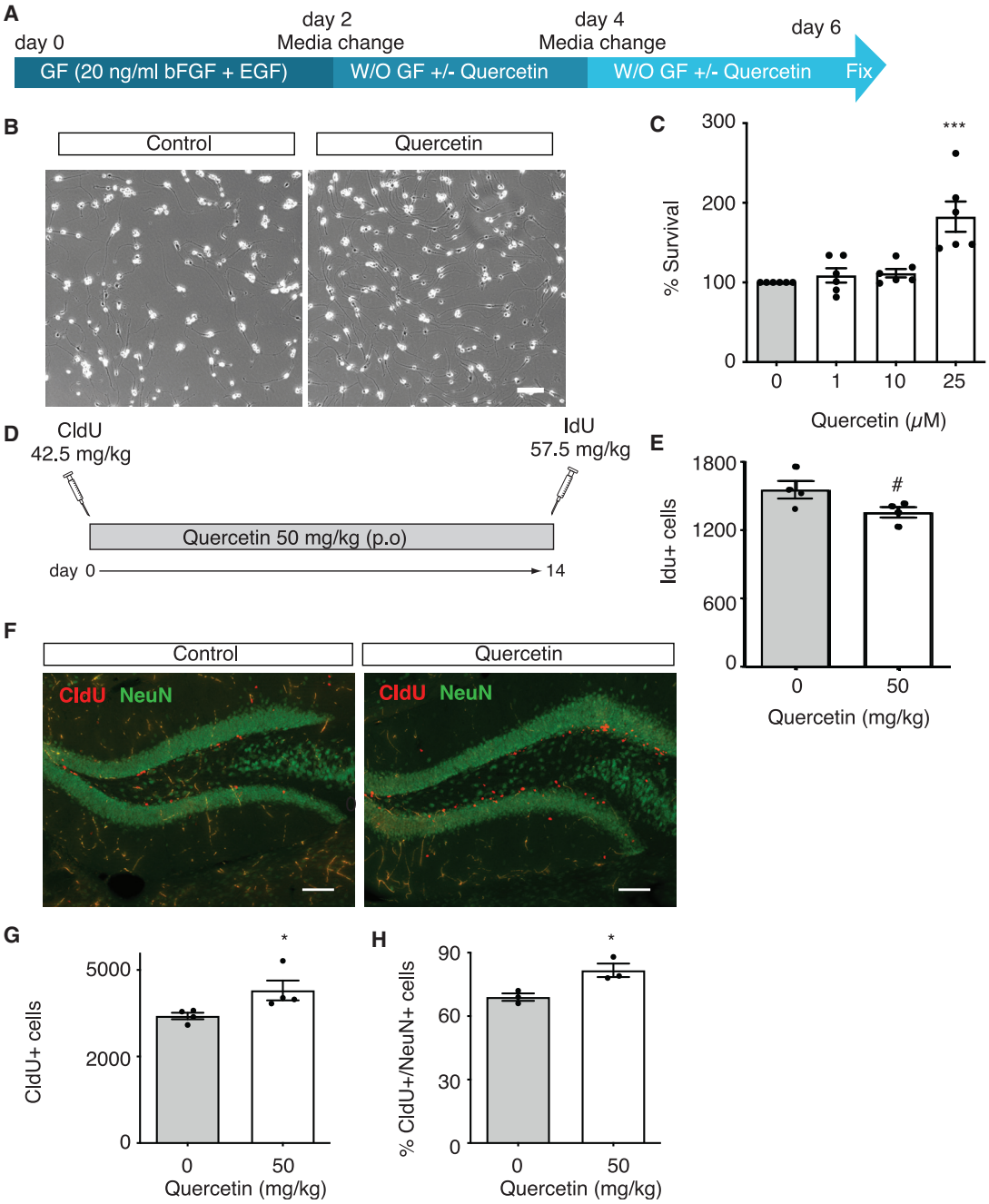

Figure 2. Quercetin Promotes *In Vitro* Cell Survival and Stimulates Adult Neurogenesis *In Vivo*

(A) Experimental scheme.

(B) Bright-field images of NPCs 96 h after growth factor withdrawal.

(C) Quercetin (25 μM) increased cell survival during differentiation. Percentage of resazurin fluorescence intensity compared with control. One-way ANOVA with Dunnett's post hoc test, n = 6 independent experiments.

(D) Experimental scheme for CldU and IdU injection and quercetin treatment.

(E–H) (E) A trend toward a decrease in IdU^+ cells was observed in the quercetin-treated animals. (F) Immunofluorescence staining shows the cohort of cells that were $CldU^+$ (red) and $NeuN^+$ (green). A significant increase in the number of $CldU^+$ (G) and $CldU^+NeuN^+$ (H) cells was observed in the quercetin-treated group. $^{\#}p = 0.068$; $^{*}p < 0.05$, $^{***}p < 0.001$, Student's t test, n = 4 mice per group. Scale bars, 50 μm.

Please cite this article in press as: Ichwan et al., Apple Peel and Flesh Contain Pro-neurogenic Compounds, Stem Cell Reports (2021), https://doi.org/10.1016/j.stemcr.2021.01.005

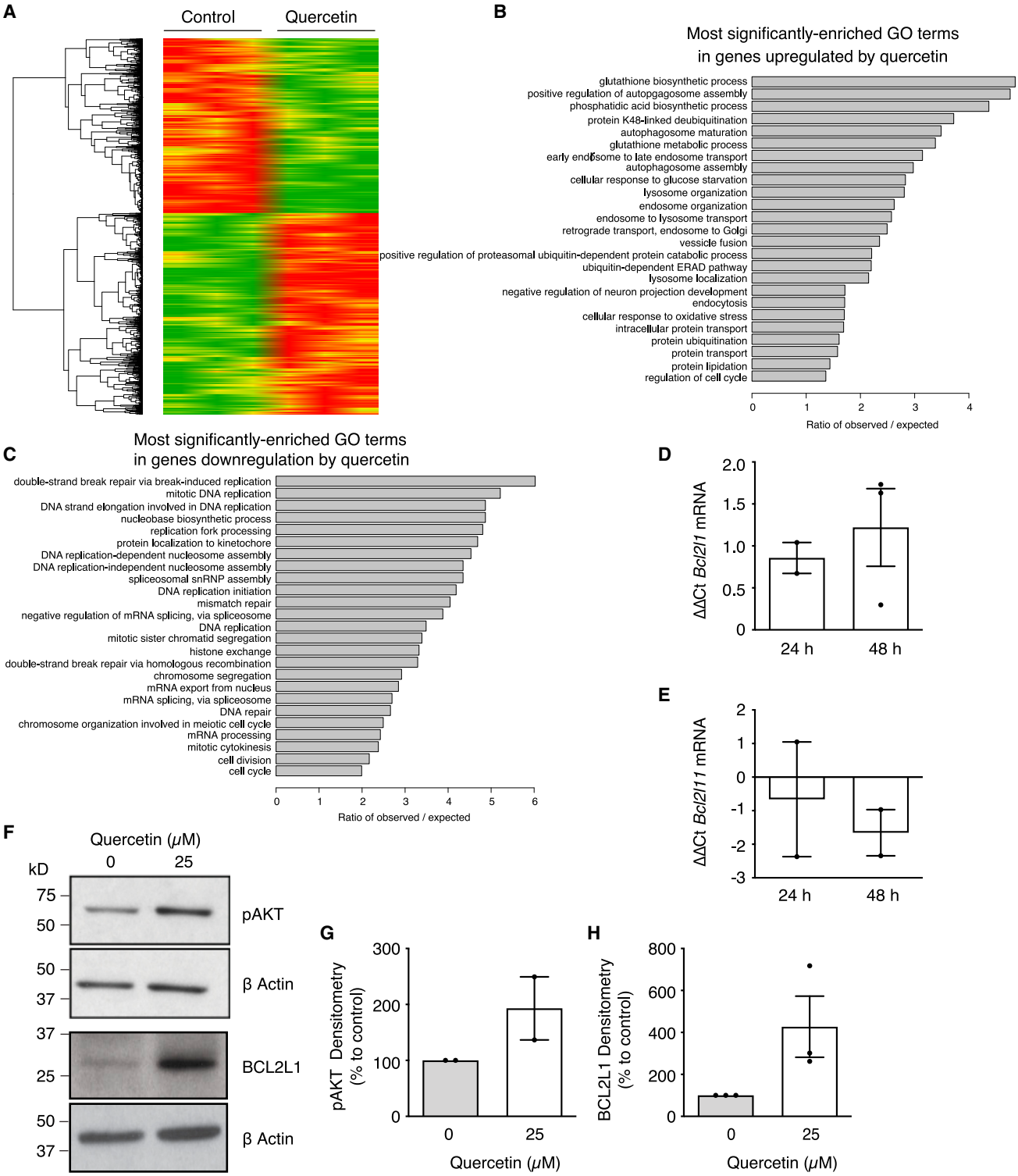

Figure 3. Quercetin Induces Endogenous Antioxidants and the AKT Pathway

(A–E) (A) A heatmap showing changes in NPC transcript expression in cells treated with 25 μM quercetin, 24 h after growth factor withdrawal. The top 25 most enriched pathways from the KEGG database for significantly upregulated (B) or downregulated (C) transcripts.

(legend continued on next page)

pathways (reviewed by Spencer, 2009). The flavonoids were reported to exert their effect on cell survival through modulation of the MAPK and phosphoinositide-3 kinase (PI3K-AKT) pathways. The enrichment analysis of the MAPK pathway showed that p42/44 extracellular signal-regulated kinase (ERK) was not differentially expressed in response to quercetin treatment. In contrast, JNK2 and JNK3 were upregulated, whereas JNK1 was downregulated. The transcripts of JNK-related proapoptotic genes, namely *Bid*, *Bax*, and *Puma*, were also upregulated in the quercetin-treated group (Table S2). To determine whether the pro-survival and anti-apoptotic signals were simultaneously upregulated, we analyzed the enrichment of the differentially expressed genes in the PI3K-AKT pathway from the KEGG database and the NRF2-Keap1 (kelch-like ECH-associated protein 1) pathway from the WikiPathways database. In the PI3K-AKT pathway we observed significant upregulation of pro-survival genes such as *Akt*, *Creb*, *Mdm2*, and *BclxL* (*Bcl2l1*). In contrast, apoptosis-inducing genes such as *p53* and *Bim* (*Bcl2l11*) were downregulated (Table S3).

To confirm the transcriptomic data, we performed qPCR to quantify the expression level of Bcl2l1 and *Bcl2l11*. Our results revealed a trend toward *Bcl2l1* upregulation over time in the quercetin-treated group (Figure 3D), but a trend toward decreased expression of the pro-apoptotic gene *Bcl2l11* (Figure 3E). Increased expression of phospho-AKT (pAKT) and BCL2l1 was also observed at the protein level. After 48 h incubation with 25 μM quercetin, pAKT expression was significantly upregulated (Figures 3F and 3G). A similar but non-significant pattern was also observed for BCL2l1 protein expression (Figures 3F and 3H). Another highly enriched pathway that potentially explains the mechanism via which quercetin promotes the survival of differentiating NPCs is the NRF2-Keap1 pathway. One of the downstream genes in this pathway, *Gsta3* (glutathione S-transferase α3), was the most highly expressed gene in differentiating NPCs upon 25 μM quercetin treatment (Table S4). In addition to *Nrf2* upregulation, the *Nrf2* antagonist *Keap1* was increased in the quercetin-treated group. This increase in *Keap1* expression may counteract the detrimental effect of excessive *Nrf2* accumulation.

Apple Peel and Flesh Are Pro-neurogenic *In Vitro*

Given the above findings with quercetin, we next wanted to determine whether apple peel or flesh displays similar pro-neurogenic properties. We first sought to identify an apple cultivar that is particularly rich in flavonoids by comparing six locally harvested varieties: Elstar, Pinova, Pilot, Rebella, Roter Berlepsch, and Jonagold. Using the borohydride-chloranil assay, we found that these varieties differed greatly in their absolute flavonoid content, although all contained flavonoids in their peel and, to a much lesser extent, in their flesh (Table S5). The enrichment in the peel was greatest (almost 9-fold) in the Pinova cultivar. Using the neurosphere assay, we found that Pinova peel (Figure 4A) and flesh extract (Figure 4A) had a similar pro-neurogenic capacity.

Apple Juice Supplementation Does Not Affect Adult Neurogenesis *In Vivo*

Given the wide consumption of apple juice, we next examined whether consumption of whole apple juice concentrate affected adult neurogenesis *in vivo*, with concomitant effects on learning and memory (Figure 4B). To exclude the effect of the increased caloric intake of fruit sugar as a potential confounding factor, a group that received equicaloric sugar water was included in addition to the control group that received normal drinking water. However, all mice showed a similar change in body weight over the experimental period (Figure 4C). Food consumption was greater in mice that drank water compared with mice that received apple juice or equicaloric sugar water (Figure 4D). Liquid consumption differed greatly between the groups, with the highest consumption in the sugar water group (Figure 4E). To detect whether the apple juice supplement had an effect on hippocampus-dependent learning, a reversal version of the Morris water maze task, designed to detect the specific contribution of adult-generated neurons to the overall performance in spatial navigation and cognitive flexibility, was performed (Garthe et al., 2009; Figure 4F). We did not detect any difference between the groups with respect to escape latency (Figure 4G), path length (Figure 4H), probe trial performance, or reversal learning (Figures 4G and 4H). Following the behavioral testing, the mice were perfused, and the number of surviving $BrdU^+$ cells was quantified. No effect of either the sugar water or the apple juice supplementation on adult hippocampal neurogenesis was observed (Figure 4I).

Apple Flesh Has Pro-neurogenic Activity

We next returned to our earlier observation that, despite the lower level of flavonoids in apple flesh, there was still as much pro-neurogenic activity as in peel extract. To identify additional pro-neurogenic compounds in apple extracts, we used a bioassay-guided fractionated approach.

Relative expression of the *Bcl2l1* gene increased (D) and the *Bcl2l11* gene decreased (E) in differentiating NPCs after 24 and 48 h quercetin (25 μM) treatment (n = 3 experiments).

(F–H) An increase in the expression of pAKT (G) and Bcl2l1 (H) following quercetin treatment was also observed at the protein level (F, western blot). One sample t test, n = 3 experiments.

Please cite this article in press as: Ichwan et al., Apple Peel and Flesh Contain Pro-neurogenic Compounds, Stem Cell Reports (2021), https://doi.org/10.1016/j.stemcr.2021.01.005

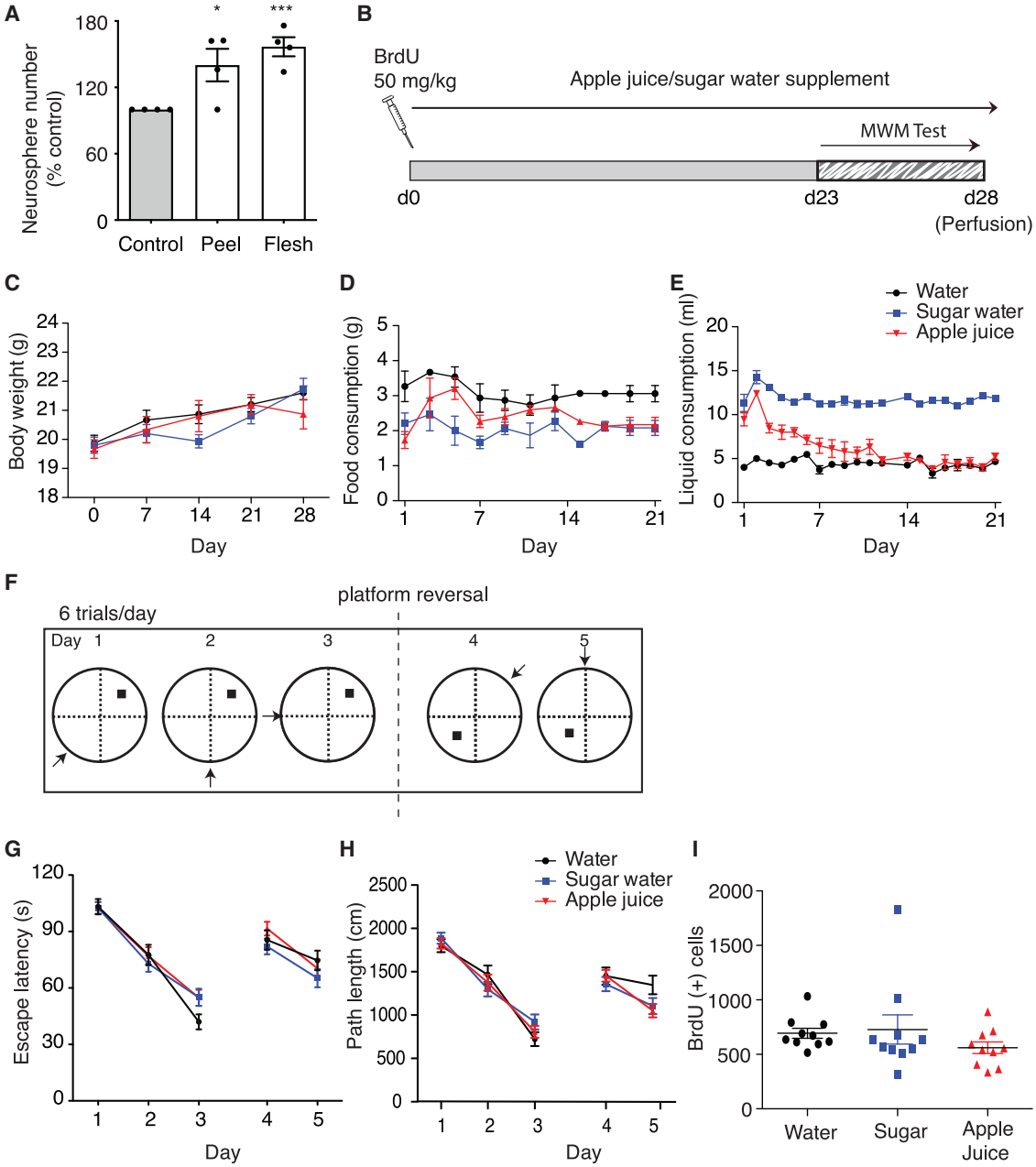

Figure 4. Apple Peel and Flesh Are Pro-neurogenic *In Vitro*, but Apple Juice Does Not Affect *In Vivo* Neurogenesis or Cognitive Function

(A) Pinova apple peel and flesh extracts significantly increased the number of primary hippocampal neurospheres. One-way ANOVA with Dunnett's post hoc test.

(B) Experimental scheme for apple juice supplementation. MWM, Morris water maze.

(C) No significant difference in body weight was observed.

(D) The water-supplemented group consumed significantly more food than the apple juice- and sugar water-supplemented mice.

(E) The sugar water-supplemented mice consumed significantly more liquid than the other groups.

(F–I) (F) Experimental scheme. No effect of apple juice or sugar water was observed based on the escape latency (G) or path length (H). No difference in the number of $BrdU^+$ cells was observed (I). One-way ANOVA, n = 10 mice per group. *$p < 0.05$, ***$p < 0.001$.

Please cite this article in press as: Ichwan et al., Apple Peel and Flesh Contain Pro-neurogenic Compounds, Stem Cell Reports (2021), https://doi.org/10.1016/j.stemcr.2021.01.005

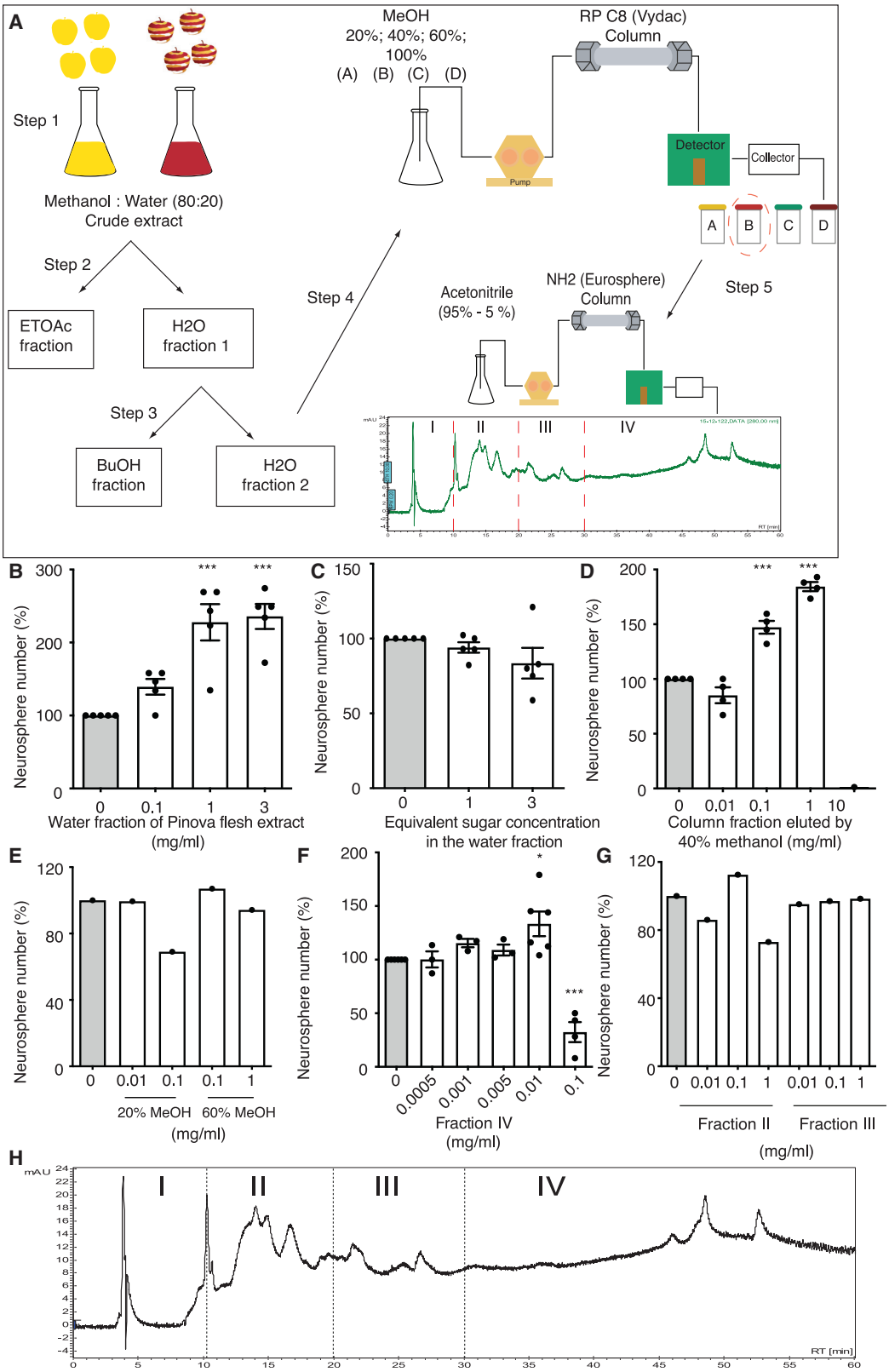

(legend on next page)

Flesh extract was separated into fractions using liquid- and solid-phase separation methods (Figure 5A). Among the three fractions (water, EtOAc, and BuOH), we found a dose-dependent increase in the number of neurospheres generated from primary dentate gyrus cell cultures in the presence of the water fraction, more than doubling the number of neurospheres (Figure 5B). The EtOAc fraction decreased neurosphere counts (0.05 mg/mL 63.2%, 0.5 mg/mL 0% of control, n = 1 experiment). Although there was a small increase in the number of neurospheres generated in the presence of the BuOH fraction (0.1 mg/mL 128% of control, n = 1 experiment), additional replicates and further fractionation steps could not be performed due to the low yield. As the water fraction also contains fruit sugar that might affect cell growth, we tested a solution with a sugar composition (sucrose, glucose, and fructose) equivalent to that of the water fraction, revealing no effect of sugar on neurosphere numbers (Figure 5C).

The water fraction was next further fractionated by high-performance liquid chromatography in solvents of different polarity (20%–100% methanol [MeOH] in water). The 40% MeOH eluent increased neurosphere number in a dose-dependent manner (Figure 5D), but decreased neurosphere counts at the high concentration of 10 mg/mL. The fractions eluted at 20% and 60% MeOH did not increase neurosphere numbers (Figure 5E) and no fraction could be obtained at 100% MeOH. The 40% MeOH fraction was fractionated into four fractions (Figures 5F–5H). The neurosphere assay revealed that fraction IV dose-dependently increased the neurosphere count, with a maximum effect at a concentration of 0.01 mg/mL (Figure 5F). At higher concentrations the number of neurospheres was again decreased. No effect of fraction II or III was observed (Figure 5G).

Fraction IV could not be further sub-fractionated because of the low amount of material. We instead used ultra-performance liquid chromatography coupled with photodiode-array detector and electrospray quadrupole time-of-flight mass spectroscopy (TOF-MS) to identify the compounds present in this fraction. The compounds eluted in the first 1.5 min could not be separated, but subsequent peaks (numbers 1–6; Figure 6A) were subjected to TOF-MS and collision-induced dissociation. Interestingly, two of the peaks were identified as the glycosides of dihydroxybenzoate (Table S6), the salt of dihydroxybenzoic acid (DHBA), which belongs to the non-flavonoid phenolic compounds present in fruits. We therefore obtained commercially available isomers of DHBA and examined their effects on NPC activity. A significant increase in neurosphere numbers was found with 2,3-DHBA at a concentration of 1 μM (Figure 6B) and 3,5-DHBA at concentrations of 1 and 10 μM (Figure 6D). Treatment with 1 μM 3,4-DHBA produced a slight increase in the number of neurospheres generated (p = 0.19; Figure 6C), whereas 10 μM 3,5-DHBA led to a significant increase in neurosphere number (Figure 6E) as well as a significant increase in neurosphere size (Figure 6F). We also found that treatment of adherent monolayer cultures with 3,5-DHBA at concentrations of 100 and 250 μM resulted in a higher cell density after 4 days in culture (Figure 6G). To determine whether this was due to 3,5-DHBA acting on NPC survival when cultured under proliferation conditions, adherent cells were cultured in growth factors for 4 days and varying concentrations of 3,5-DHBA were added on day 0 (4 day), day 2 (2 day), or day 3 (1 day), after which the resazurin cell viability assay was performed on day 4 (Figure 6H). Our results revealed an increase in the percentage of cell survival at the higher 3,5-DHBA concentrations, with the strongest effect size observed when the 3,5-DHBA was present in the medium for the entire 4 days of the experiment (Figures 6I–6K). We also examined whether 3,5-DHBA had a similar cell survival effect when the adherent NPCs were cultured under differentiation conditions (Figure 6L). Again we observed a neuroprotective effect, with a significant increase in cell survival found in the cells treated with 3,5-DHBA (≥250 μM) throughout the entire differentiation process (Figure 6M). After 6 days of differentiation these cells were fixed and stained for markers of mature neurons and astrocytes. We found a significantly higher percentage of βIII-tubulin$^+$ neurons in the cultures differentiated in the presence of high concentrations of 3,5-DHBA, further confirming its pro-neurogenic effect (Figures 6N and 6O).

HCAR1, the Putative Receptor for Hydroxybenzoic Acid, Is Expressed on NPCs and in the Neurogenic Niche *In Vivo*

The hydroxycarboxylic acid receptor 1 (HCAR1) had been listed as an orphan receptor until it was identified as the

Figure 5. Apple Flesh Extracts Display Pro-neurogenic Activity

(A) Experimental scheme for the extraction and fractionation of apple extract.

(B–H) (B) The water fraction of Pinova flesh extract significantly increased the number of hippocampal neurospheres, whereas (C) the equivalent concentration of sugar had no effect; n = 5 independent experiments. Following further separation of the water fraction, (D) the 40% methanol-eluted fraction significantly increased the number of hippocampal neurospheres (n = 4 experiments), whereas (E) the 20% and 60% methanol fractions had no effect (n = 1 experiment). Following further fractionation of the 40% methanol fraction, the pro-neurogenic activity was restricted to fraction IV (F, fraction IV; G, fractions II and III; n = 3 individual experiments; H, HPLC elution trace). One-way ANOVA with Dunnett's post hoc test. *p < 0.05, ***p < 0.001.

Please cite this article in press as: Ichwan et al., Apple Peel and Flesh Contain Pro-neurogenic Compounds, Stem Cell Reports (2021), https://doi.org/10.1016/j.stemcr.2021.01.005

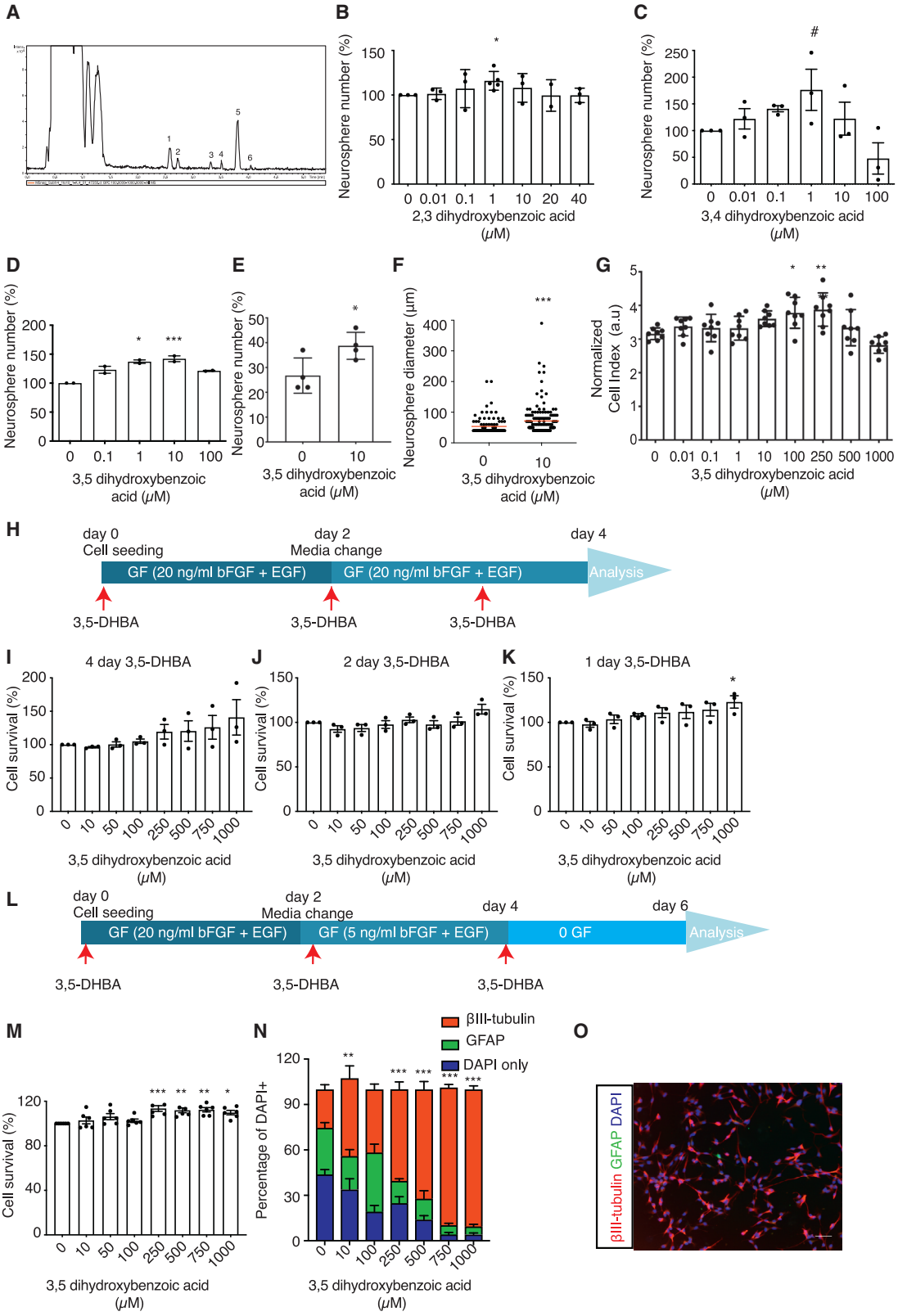

(legend on next page)

receptor for lactate and 3,5-DHBA. HCAR1 is expressed in the brain, including in the hippocampus (Castillo et al., 2015). Using immunocytochemistry we confirmed that HCAR1 was expressed by proliferating nestin$^+$/Sox2$^+$ hippocampal adherent monolayer cells *in vitro* (Figure 7A). Immunofluorescence staining of brain sections revealed that, in addition to being expressed by the granular cells of the dentate gyrus, as has been previously reported (Castillo et al., 2015), HCAR1 is also expressed by type 1 and type 2 NPCs, as evidenced by the co-expression of nestin and Sox2 (Figure 7B).

3,5-DHBA Increases NPC Proliferation and Neurogenesis *In Vivo*

Given the positive effects of 3,5-DHBA on NPC proliferation and survival *in vitro*, and the presence of HCAR1 on NPCs *in vivo*, we finally examined whether administration of 3,5-DHBA affects *in vivo* NPC proliferation and adult neurogenesis. To do this, 3,5-DHBA (15.625, 31.25, 62.5, 125, and 250 mg/kg) was administered intraperitoneally to adult mice once daily for 14 days prior to perfusion. A group that received no DHBA, but had free access to a running wheel, was included as a positive control. All mice received two intraperitoneal injections of BrdU (50 mg/kg) spaced 1 h apart prior to the first dose of 3,5-DHBA to label the proliferating cells. Treatment with 3,5-DHBA resulted in a significant increase in the number of proliferating NPCs in the subgranular zone of the dentate gyrus in all but the group receiving the highest dose of 3.5-DHBA, with the greatest effect being observed at a dose of 62.5 mg/kg (Figures 7C and 7D). A similar result was observed following quantification of the number of BrdU-labeled cells (Figures 7E and 7F). Finally, the number of immature neurons (DCX$^+$) was counted to determine whether, in addition to proliferation, 3,5-DHBA treatment also influences adult neurogenesis. Similar to the results obtained for the *in vitro* experiments, we observed a significant increase in the number of newborn neurons in all but the group receiving the highest dose of 3,5-DHBA, with the greatest increase observed in the group receiving 62.5 mg/kg (Figures 7G and 7H). To examine whether 3,5-DHBA treatment also affected the maturation rate of the newborn neurons, the DCX$^+$ cells were morphologically categorized according to the presence and shape of their apical dendrites (Plumpe et al., 2006). Briefly, category A and B cells had no or very short processes, C and D cells had increasingly longer processes that, by stage D, had reached the molecular layer, and category E cells had one strong dendrite with sparse branching, whereas in category F cells the dendritic tree was more elaborate, with multiple branches in the molecular cell layer. We found that the mice treated with 62.5 mg/kg 3,5-DHBA had both a significantly higher percentage and a significantly higher absolute number of DCX$^+$ cells belonging to categories E and F than the control mice, indicating that 3,5-DHBA treatment increases the maturation speed of the newly born neurons (Figures 7I and 7J). Interestingly, and consistent with our previous report (Plumpe et al., 2006), this change in dendritic morphology was not observed in the positive control group of mice that exercised.

DISCUSSION

In this study we demonstrate that apples contain pro-neurogenic compounds in both their peel and their flesh. Our data reveal that, while quercetin is anti-proliferative at high concentrations, its effect on NPCs at lower concentrations is more complex and appears to involve activation rather than inhibition. We found that 25 μM quercetin

Figure 6. Hydroxybenzoic Acid Is a Pro-neurogenic Compound Found in Apple Flesh

(A–E) (A) Base peak chromatogram m/z 100–1000, gradient elution, electrospray ionization(−) of fraction IV. Six peaks. were annotated, two of which (peaks 2 and 4) were glycosides of dihydrobenzoate. Neurosphere assays revealed that the dihydroxybenzoic acid isomers (B) 2,3-DHBA, (C) 3,4-DHBA, and (D and E) 3,5-DHBA all increased precursor proliferation, with the greatest effect observed in response to 3,5-DHBA. n = 2–5 individual experiments. $^{\#}p = 0.19$.

(F) In addition to increasing neurosphere number, 3,5-DHBA also significantly increased the diameter of the resulting neurospheres.

(G) Using the xCELLigence impedance-based assay, an increased number of cells were detected in adherent monolayer cultures treated with 100 and 250 μM 3,5-DHBA. n = 8 independent experiments.

(H) Adherent cells were cultured in 20 ng/mL epidermal growth factor (EGF) and basic fibroblast growth factor (bFGF) for 4 days and varying concentrations of 3,5-DHBA were added on day 0, 2, or 3. The resazurin assay was then performed on day 4.

(I–K) An increase in the percentage of cell survival at the higher 3,5-DHBA concentrations was observed. (I) 4 day, (J) 2 day, (K) 1 day. n = 3 independent experiments.

(L) Adherent precursor cells were cultured under differentiation conditions with 3,5-DHBA present throughout the experiment.

(M) A significant increase in cell survival was observed in the differentiating cells treated with ≥250 μM 3,5-DHBA. n = 6 independent experiments.

(N and O) (N) 3,5-DHBA dose-dependently increased the number of surviving differentiated neurons, with the highest effect observed (O) in the cultures treated with 1,000 μM 3,5-DHBA.

One-way ANOVA with Dunnett's post hoc and Student's t test (E and F). Scale bar in (O), 50 μm. $^*p < 0.05$, $^{**}p < 0.01$, $^{***}p < 0.001$.

Please cite this article in press as: Ichwan et al., Apple Peel and Flesh Contain Pro-neurogenic Compounds, Stem Cell Reports (2021), https://doi.org/10.1016/j.stemcr.2021.01.005

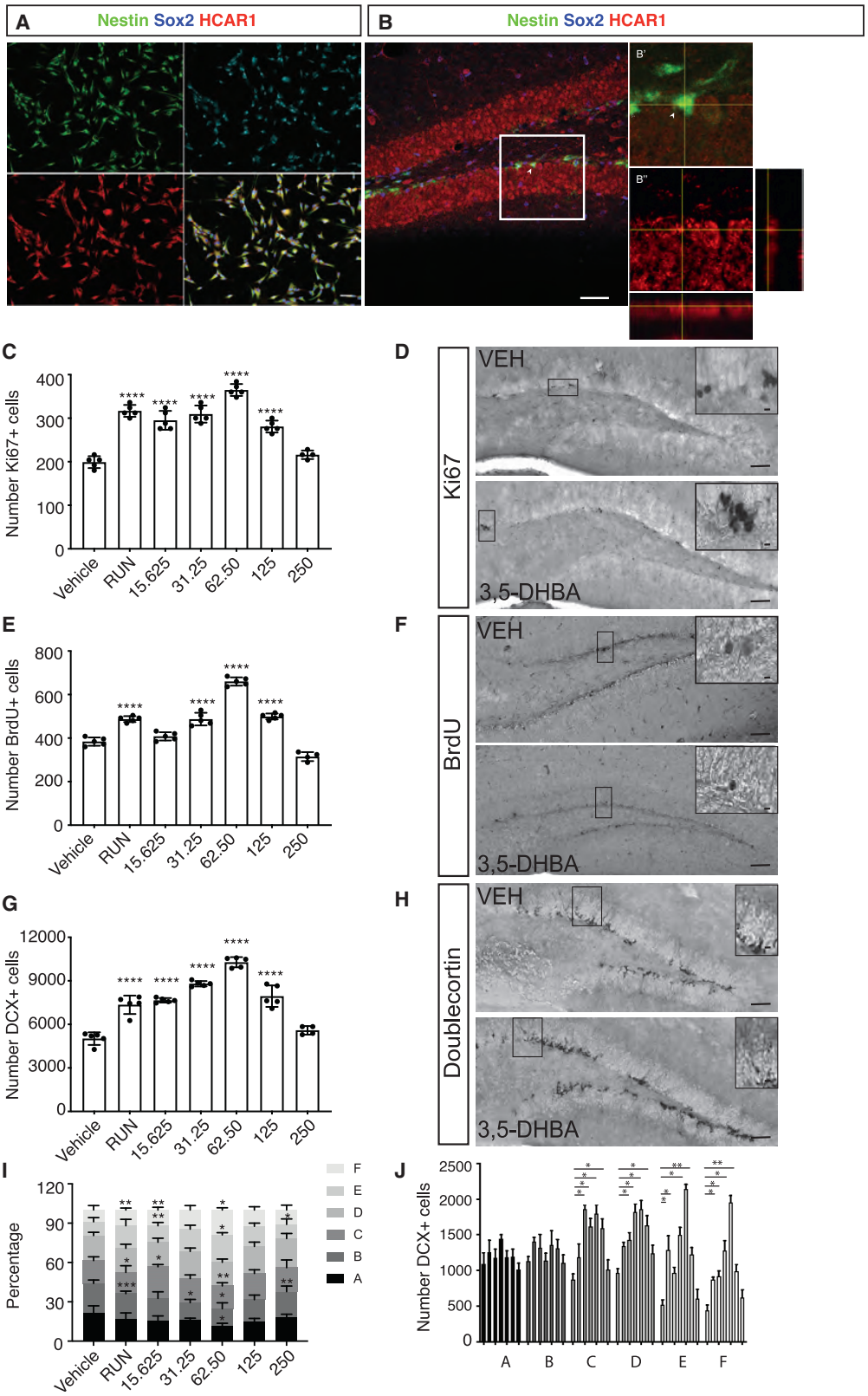

(legend on next page)

increased cell-cycle exit and promoted the survival and differentiation of adult hippocampal NPCs, both *ex vivo* and *in vivo*. This is similar to the effect that we and others have previously reported for compounds such as resveratrol and EGCG (Ortiz-Lopez et al., 2016; Torres-Perez et al., 2015; Yoo et al., 2010). Natural compounds such as these, which are abundant in widely consumed fruits and vegetables, might therefore contribute to a beneficial effect on neurogenesis and brain function as part of broader environmental influences.

Based on transcriptomic data we propose that the PI3K-AKT and NRF2-KEAP1 pathways are involved in such effects. This is in agreement with previous reports that flavonoids have numerous modes of action. Under stress conditions, there is an activation and accumulation of NRF2 in the nucleus (Nguyen et al., 2009). The heterodimer of NRF2 with small MAF (musculoaponeurotic fibrosarcoma) has been shown to increase the binding affinity with ARE, which leads to the transcription of phase II enzymes (Itoh et al., 1997). These enzymes play important roles in endogenous protection systems by neutralizing the harmful by-products of oxidative stress (Nguyen et al., 2003). A downstream gene in this pathway, *Gsta3*, was the most highly expressed gene in differentiating NPCs after 25 μM quercetin treatment. In addition to *Nrf2* upregulation, *Keap1* was also upregulated in the quercetin-treated group. This protein facilitates the nucleocytoplasmic shuttling mechanism of Nrf2 and subsequently promotes its ubiquitinoylation and degradation (Nguyen et al., 2005). Bell and colleagues demonstrated that the overexpression of NRF2 inhibits neurite outgrowth and neuronal maturation (Bell et al., 2015). It is therefore likely that the upregulation of KEAP1 expression in response to quercetin treatment counteracts the detrimental effect of excessive NRF2 accumulation.

Given the pro-neurogenic nature of quercetin, we sought to determine whether apple extracts display similar properties. We found that apple extracts from the flesh and to a lesser extent the peel increased neurosphere formation *in vitro*. Previous studies in aged animals found that apple supplementation prevented oxidative brain damage through increased endogenous antioxidative capacity, as well as restoring long-term potentiation and acetylcholine level, concurrent with improvement in behavioral tasks (Tchantchou et al., 2005; Viggiano et al., 2006). A pilot human study showed that the consumption of apple juice improved behavioral symptoms in patients with Alzheimer's disease (Remington et al., 2010). However, no significant cognitive change was observed after short-term apple supplementation in healthy volunteers (Bondonno et al., 2014). We therefore investigated whether apple juice consumption could increase neurogenesis and enhance spatial learning and memory in mice. Despite observing pro-proliferative effects of apple extract *in vitro*, we found no effect of apple juice consumption on *in vivo* neurogenesis or spatial learning and memory performance. Given that the quercetin concentration in apple juice is very low (below 2 mg/L), resulting in an intake of approximately 0.6 mg/kg, we conclude that this is likely an insufficient concentration of active phytochemical to modulate neurogenesis with a measurable effect size. This, however, does not exclude a contributing effect to overall environmental effects on brain function.

Interestingly, we identified DHBA as a pro-neurogenic factor unrelated to flavonoids. Hydroxybenzoic acid is abundant in fruits, where it acts as a natural preservative (Soni et al., 2005). Multiple bioactive molecules are structurally related to 3,5-DHBA (Hubkova et al., 2014), some of which (e.g., 3-HBA) also bind to the HCA2 receptor, whereas 3,5-DHBA specifically, albeit weakly, binds to HCAR1 (Liu et al., 2012). Interestingly, HCAR1 is a Gi-coupled receptor, which, after activation, inhibits adenylate cyclase to downregulate formation of cyclic adenosine monophosphate (cAMP) (Liu et al., 2012). Biochemical studies have revealed that 3,5-DHBA shows a higher potency to decrease the levels of cAMP in SK-N-MC cells than lactate, the natural ligand of HCAR1 (Liu et al.,

Figure 7. 3,5-DHBA Increases Neural Precursor Cell Proliferation and Neurogenesis *In Vivo*

(A) Immunofluorescence staining of proliferating adult hippocampal precursor cells in monolayer culture. HCAR1 (red) co-localized with the neural precursor cell markers nestin (green) and Sox2 (cyan).

(B–H) (B) Confocal z-stack image of the hippocampal dentate gyrus in brain sections from nestin-GFP mice. HCAR1 (red), nestin (green), and Sox2 (dark blue). Arrowhead points to a nestin$^+$ cell with HCAR1 co-localization confirmed in orthogonal view (B″). *In vivo* administration of 3,5-DHBA resulted in a significant increase in the number of proliferating (Ki67$^+$) cells (C, D), BrdU$^+$ cells (E, F), and DCX$^+$ immature neurons (G, H) in the dentate gyrus. n = 5 animals per group.

(I) 3,5-DHBA administration altered the dendritic morphology of the newly born neurons, increasing the percentage of DCX$^+$ cells with a more mature phenotype.

(J) 3,5-DHBA administration also increased the absolute number of DCX$^+$ cells with a mature morphology (DCX classes C–F). For each DCX$^+$ cell class the bars are vehicle, RUN, and 15.625, 31.25, 62.5, 125, and 250 mg/kg 3,5-DHBA from left to right.

One-way ANOVA with Dunnett's post hoc test in (C, E, and G) and two-way ANOVA with Tukey post hoc test in (I and J). Scale bars, 150 μm and, for the insets, 15 μm. *$p < 0.05$, **$p < 0.01$, ***$p < 0.001$, ****$p < 0.0001$.

2012). 3,5-DHBA is also more potent than lactate in hippocampal slices (Liu et al., 2012).

Although the food industry uses benzoic acid as a preservative, naturally occurring DHBA has received relatively little attention as a potential signaling molecule. DHBA binds to the lactate receptor, GPR81/HCAR1 (Cai et al., 2008), which, as we show, is present on NPCs, suggesting a direct mode of action. At the same time, given the role of lactate as both a signaling molecule and a source of energy for neurons, the discovery of an intrinsically active agonist to the receptor on neural stem cells is of further relevance (Lev-Vachnish et al., 2019; Wang et al., 2019). We found that 3,5-DHBA not only increases NPC proliferation and neurogenesis, but also increases the maturation rate of these newborn cells. This appeared to be a concentration-dependent effect, with the most effective dose being 62.5 mg/kg and no effect observed at the highest concentration tested (250 mg/kg). In accordance with our results, another study also observed that administration of high concentrations of 3,5-DHBA had no effect on the long-term survival of newly born neurons (Lev-Vachnish et al., 2019). However, in that study lower concentrations of DHBA were not examined. Thus, the observation of a dose-dependent response to 3,5-DHBA is interesting, as it might indicate differential regulation and a modulatory effect. Little is known about downstream signaling events after HCAR1 activation. However, in muscle myotubes, 3,5-DHBA has been shown to stimulate phosphorylation of MAPK kinase 1/2 (MEK1/2), ERK1/2, and p90 ribosomal S6 kinase (p90RSK) (Ohno et al., 2018). In hippocampal neurons, 3,5-DHBA also affects energy metabolism, ion homeostasis, and (possibly directly) synaptic signaling (Angamo et al., 2016).

We have shown that both flavonoids and DHBA are pro-neurogenic, not only by activating NPC proliferation but also by promoting cell-cycle exit, cellular survival, and neuronal differentiation. An obvious caveat of our approach is the limitation of the *in vitro* experiment. Both quercetin and isoforms of DHBA have been used as targeting moieties to facilitate drug delivery across the blood-brain barrier (Guo et al., 2020; Pinto et al., 2020). Therefore, although our *in vivo* experiments cannot distinguish direct from indirect effects, the *ex vivo* studies indicate that direct effects are generally possible.

EXPERIMENTAL PROCEDURES

Animals

Male and female C57BL/6JRj mice were purchased from Janvier and experiments were conducted in accordance with the applicable European (86/609/EEC) and national (Tierschutzgesetz) regulations and approved by the local ethics committee (DD24-5131/207/27). The C57BL/6NHsd mice were purchased from Harlan Laboratories (Mexico City) and BALB/c mice were obtained from the animal facility of the National Institute of Psychiatry "Ramón de la Fuente Muñiz," with experiments conducted in accordance with the national regulations (NOM-062-ZOO-1999) and approved by the local ethics committee (CEI/C/009/2013). Mice were housed in standard laboratory cages (4 or 5 mice per cage) under a 12 h light/12 h dark cycle at a temperature of 23°C ± 1°C. The animals had *ad libitum* access to food and water.

In Vivo Quercetin Treatment

CldU (42.5 mg/kg) was injected at the beginning of the experiment and IdU (57.5 mg/kg) was injected 2 h before the animals were perfused with 4% paraformaldehyde (PFA). Quercetin (50 mg/kg; Sigma) was prepared fresh in propylene glycol and administered daily through oral gavage (total volume 200 μL).

In Vivo Apple Juice Supplementation

Pinova apples were purchased from Obsthof Schlage Dresden-Pillnitz, harvested in autumn 2014. Eight liters of apple juice was obtained from 13 kg of fresh apples, then aliquoted, and stored at −80°C. Mice were housed in groups of five that received juice, sugar water, or normal drinking water. The sugar water or apple juice was replaced daily. Food and liquid intake was measured daily and body weight was measured weekly. A single injection of BrdU (50 mg/kg) was given on the first day of the experiment and the mice were perfused 1 day after the completion of the water maze task.

Isolation of Adult Hippocampal Neural Precursor Cells

The isolation procedure for adult hippocampal NPCs was adapted from Babu et al. (2007). Mice were killed by cervical dislocation, the brains were collected, and the dentate gyrus was dissected as previously described (Walker and Kempermann, 2014). The tissue was dissociated using a Neural Dissociation Kit-P (Miltenyi Biotec) and the cells were resuspended in 1 mL of growth medium (Neurobasal medium containing 2% B27 supplements, 1× GlutaMAX, 2 μg/mL heparin, 50 units/mL penicillin/streptomycin, 20 ng/mL epidermal growth factor (EGF) and 20 ng/mL basic fibroblast growth factor (bFGF-2)). The cells were then plated into one well of a PDL- and laminin-coated 12 well plate and incubated in 37°C, 5% CO_2, for monolayer cultures, or into an uncoated 96 well plate for neurosphere cultures. The tested compounds/extracts were dissolved in water or DMSO, depending on the solubility. When DMSO was used as the vehicle, the final concentration in the culture medium did not exceed 0.1% and an equivalent volume of DMSO was added to control conditions.

Adherent Monolayer Cell Culture

Five or six male and female C57BL/6JRj mice were used to establish a monolayer culture. After tissue dissociation, the NPCs were plated into a PDL/laminin-coated plate and incubated at 37°C with 5% CO_2. Every second day, half of the medium was replaced with fresh proliferation medium containing 20 ng/mL bFGF and 20 ng/mL EGF. After reaching 80% confluency, the cells were passaged and replated at a density of 10,000 cells/cm^2. This was repeated until passage 6, after which the cells were cryopreserved in vials each containing 1 × 10^6 cells. For each of the adherent

monolayer culture experiments, a vial of stock cells was thawed and plated into a T25 flask containing proliferation medium. The cells were passaged at least once before being plated into at least three replicate wells of a PDL/laminin-coated 24 well plate and treated as described in each individual experiment. This constituted an n = 1 and was repeated an additional three or four times on subsequent passages to provide the data described as n = 3 or 4 individual experiments for each dataset. The cells used for experiments did not exceed passage 15.

Neurosphere Assay

Freshly isolated NPCs from the dentate gyrus were resuspended in complete neurosphere medium to reach the approximate density of two hippocampi in 10 mL medium, and subsequently filtered through a 40 μm nylon mesh cell strainer (Walker and Kempermann, 2014). After the test compounds or vehicle was added, the cells were plated in a 96 well plate and incubated at 37°C, 5% CO_2 for 12 days. Neurospheres with diameters ≥ 40 μm were counted using an inverted light microscope.

Cell-Cycle Analysis with Propidium Iodide Staining

Cells were harvested and fixed with ice-cold 70% ethanol. Following two PBS washes, the cell pellet was treated with 50 μL RNase A (100 μg/mL). Subsequently, 400 μL propidium iodide solution (50 μg/mL solution) was then added and the cells were incubated for 1 h in the dark prior to flow cytometric analysis.

7-Aminoactinomycin D Cell Death Assay

Cells were harvested into 15 mL falcon tubes and washed twice with PBS. The cell pellet was resuspended in 400 μL PBS and treated with 20 μL (1 μg) of 7-aminoactinomycin D solution. As the positive control, 0.2% Triton X-100 was added to the cell solution. Flow cytometric analysis was performed following a 10 min incubation.

In Vitro BrdU Labeling and Immunostaining

Cells were plated on PDL/laminin-coated glass coverslips in 24 well plates at 10,000 cells/cm^2 and incubated in proliferation medium for 48 h. The medium was replaced with fresh proliferation medium containing test compounds or vehicle (DMSO) and incubated for another 24 h. BrdU (10 μM) was applied for 2 h prior to fixation. The cells were fixed with 4% PFA for 10 min and subsequently washed three times with PBS prior to being stained. See Supplemental Experimental Procedures for a detailed staining procedure.

Fluorescence and DAB Immunostaining on Brain Tissue

Mice were deeply anesthetized by intraperitoneal injection of xylazine and ketamine and subsequently perfused with 0.9% NaCl and 4% PFA. The brains were collected and immersed in 4% PFA solution for 24 h, after which they equilibrated in 30% sucrose. Serial coronal cryosections (40 μm) were cut using a microtome (Leica) and stored in cryoprotection solution at −20°C. Every sixth section of each brain was pooled in one series and stained using standard protocols. See Supplemental Experimental Procedures for a detailed procedure and Table S7 for a list of antibodies used.

Resazurin Survival Assay

Cells were incubated in 0.05 mM resazurin dye (7-hydroxy-3H-phenoxazin-3-one 10-oxide) for 2 h at 37°C and the fluorescence intensity was then measured in a plate reader at 560 nm ex/590 nm em filter settings.

Western Blot

Cells were collected in lysis buffer with protease inhibitor cocktail and disrupted by trituration using a syringe fitted with a 20G needle. The proteins were separated by SDS-PAGE and transferred to nitrocellulose membranes. The membranes were blocked and then probed with primary antibodies and horseradish peroxidase-labeled secondary antibodies. Protein bands were detected using a horseradish peroxidase/chemiluminescence system (ECL Western Blotting Substrate, Pierce) and visualized on Hyperfilm ECL (Amersham). The films were scanned and band intensities were determined using ImageJ (http://imagej.nih.gov/ij/).

RNA Microarray

The total RNA from monolayers treated with quercetin was prepared using the Qiagen RNeasy mini kit. The total RNA from primary cells treated with apple extract was prepared using the Qiagen RNeasy micro kit, followed by an amplification step using Ovation Pico and PicoSL WTA System V2 and Encore biotin module. RNA samples were amplified using the TotalPrep RNA amplification kit (Illumina) and hybridized to MouseWG-6 v.2.0 Expression BeadChips (Illumina). Raw data were preprocessed with quantile normalization in R/Bioconductor using the package beadarray. The array was reannotated by querying each probe sequence against the mm9 mouse genome using the BLAT algorithm (kindly supplied by Dr. Jim Kent; http://hgwdev.cse.ucsc.edu/~kent/exe/linux). The genomic position of probes returning a single hit was then used to assign the probe to an NCBI Entrez Gene ID. Probes targeting the same gene ID were collapsed as a means to yield data for 21,155 unique genes. Using the Benjamini-Hochberg method, the gene expression result was corrected with adjusted $p < 0.05$ as the significance cutoff and then visualized using a volcano plot. The gene expression was presented as "expression relative to control," which was the result of log2 fold change. The value 1 indicates a 2-fold change of differentially upregulated expression and −1 indicates a 2-fold change of differentially downregulated expression. The list of differentially expressed genes was enriched into KEGG pathways (Kanehisa and Goto, 2000) and WikiPathways (Kelder et al., 2009) using WebGestalt, a web-based gene enrichment analysis tool.

Real Time PCR

Adherent cultures were washed with PBS and harvested in RLT buffer. Total RNA was prepared using the Qiagen RNeasy mini kit. The cDNA was prepared from 1 μg of RNA using Superscript II kit and oligo(dT) primers. qPCR analysis was performed using SYBR Green PCR Mix (Qiagen). Thermal cycling and fluorescence analysis were performed using the ΔΔCt method after normalizing to the β-actin gene. See Table S8 for a list of primer sequences.

Apple Extraction

The extract was prepared from the Pinova apple cultivar, which was obtained from a local apple orchard (Obstgut Dreßler Sobrigau, Kreischa) (Schlage Obsthof) in autumn 2011. The apple peel (100 g fresh weight) and flesh (200 g fresh weight) were separately blended in 200 mL 80% MeOH and then filtered through Whatman filter paper grade 1. The process was repeated three times. The solution was then centrifuged for 10 min, 6,000*g* at 4°C. The supernatant was collected and dried in a rotary evaporator at 40°C prior to being fractionated (see Supplemental Experimental Procedures for details on the fractionation process and total flavonoid assay).

Morris Water Maze

Three weeks after apple juice supplementation, mice were trained to locate a submerged escape platform in a circular pool (2 m diameter). The water was made opaque with non-toxic titanium dioxide and kept at a temperature of 19°C to 20°C. Each mouse underwent six trials a day for 5 consecutive days. On day 4 the position of the platform was changed to the opposite quadrant (reversal). The starting position was changed every day and remained constant for all trials each day. Mice were allowed to search for the platform for up to 120 s. At the end of each trial, they were guided to the platform and allowed to remain there for 15 s. The first 30 s on the first trial of day 4 was used as the probe trial. Swim paths were recorded using Ethovision (Noldus) and further analyzed using MatLab (MathWorks, USA).

In Vivo 3,5-DHBA Treatment

3,5-DHBA was prepared fresh every day and dissolved in 5% ethanol in 0.9% NaCl to administer at doses of 15.625, 31.25, 62.5, 125, and 250 mg/kg body weight to female Balb/c mice. 3,5-DHBA was administered once daily for 14 days via intraperitoneal injection. One hour prior to the first 3,5-DHBA administration, mice received two BrdU injections (50 mg/kg), separated by 1 h.

Statistical Analysis

Statistical analysis was performed using GraphPad Prism software (v.5.0, GraphPad Software). Microarray data analysis was performed using R for Mac OS X (3.1.1). The false discovery rate method was applied to perform multiple comparison tests on the microarray data. All data are shown as means with SEM. In figures the significance levels are denoted as *$p < 0.05$, **$p < 0.01$, ***$p < 0.001$, and ****$p < 0.0001$.

Data and Code Availability

The microarray expression dataset used for analysis, as well as the raw data files, has been deposited in the GEO repository (http://www.ncbi.nlm.nih.gov/geo/) under accession GSE150803.

SUPPLEMENTAL INFORMATION

Supplemental information can be found online at https://doi.org/10.1016/j.stemcr.2021.01.005.

AUTHOR CONTRIBUTIONS

Conceptualization, M.I., G.B.R.-R., and G.K.; investigation, M.I., T.L.W., Z.N., J.L-M., C.B., V.S.A., M.B., E.A.L., L.O.L, and A.M.S.; formal analysis, R.W.O.; writing – original draft, M.I., T.L.W., and G.K.; writing – review & editing, M.I., T.L.W., G.K., G.B.R.-R, and R.W.O.; funding acquisition, M.I., G.K., N.H., G.B.R.-R, and T.L.W.; supervision, T.L.W., G.K., and G.B.R.-R.

ACKNOWLEDGMENTS

This project was funded by the Deutsche Akademischer Austauschdienst, Deutsche Forschungsgemeinschaft Sonderforschungsbereich 655, Bundesministerium für Bildung und Forschung, Consejo Nacional de Ciencia y Tecnología (CONACYT, México; grant 147377), NIPRFM (SIC 2000), and the Brazil Family Foundation for Neurology.

Received: July 20, 2020
Revised: January 10, 2021
Accepted: January 12, 2021
Published: February 11, 2021

REFERENCES

Angamo, E.A., Rosner, J., Liotta, A., Kovacs, R., and Heinemann, U. (2016). A neuronal lactate uptake inhibitor slows recovery of extracellular ion concentration changes in the hippocampal CA3 region by affecting energy metabolism. J. Neurophysiol. *116*, 2420–2430.

Aprea, J., Prenninger, S., Dori, M., Ghosh, T., Monasor, L.S., Wessendorf, E., Zocher, S., Massalini, S., Alexopoulou, D., Lesche, M., et al. (2013). Transcriptome sequencing during mouse brain development identifies long non-coding RNAs functionally involved in neurogenic commitment. EMBO J. *32*, 3145–3160.

Babu, H., Cheung, G., Kettenmann, H., Palmer, T.D., and Kempermann, G. (2007). Enriched monolayer precursor cell cultures from micro-dissected adult mouse dentate gyrus yield functional granule cell-like neurons. PLoS One *2*, e388.

Bell, K.F., Al-Mubarak, B., Martel, M.A., McKay, S., Wheelan, N., Hasel, P., Markus, N.M., Baxter, P., Deighton, R.F., Serio, A., et al. (2015). Neuronal development is promoted by weakened intrinsic antioxidant defences due to epigenetic repression of Nrf2. Nat. Commun. *6*, 7066.

Bhagwat, S., Haytowitz, D.B. (2016). USDA Database for the Flavonoid Content of Selected Foods. Release 3.2 (November 2015). Nutrient Data Laboratory, Beltsville Human Nutrition Research Center, ARS, USDA.

Bondonno, C.P., Downey, L.A., Croft, K.D., Scholey, A., Stough, C., Yang, X., Considine, M.J., Ward, N.C., Puddey, I.B., Swinny, E., et al. (2014). The acute effect of flavonoid-rich apples and nitrate-rich spinach on cognitive performance and mood in healthy men and women. Food Funct. *5*, 849–858.

Cai, T.Q., Ren, N., Jin, L., Cheng, K., Kash, S., Chen, R., Wright, S.D., Taggart, A.K., and Waters, M.G. (2008). Role of GPR81 in lactate-mediated reduction of adipose lipolysis. Biochem. Biophys. Res. Commun. *377*, 987–991.

Castillo, X., Rosafio, K., Wyss, M.T., Drandarov, K., Buck, A., Pellerin, L., Weber, B., and Hirt, L. (2015). A probable dual mode of action for both L- and D-lactate neuroprotection in cerebral ischemia. J. Cereb. Blood Flow Metab. *35*, 1561–1569.

Dillard, C.J., and German, J.B. (2000). Phytochemicals: nutraceuticals and human health. J. Sci. Food Agric. *80*, 1744–1756.

Garthe, A., Behr, J., and Kempermann, G. (2009). Adult-generated hippocampal neurons allow the flexible use of spatially precise learning strategies. PLoS One *4*, e5464.

Georgiev, V., Ananga, A., and Tsolova, V. (2014). Recent advances and uses of grape flavonoids as nutraceuticals. Nutrients *6*, 391–415.

Guo, H., Wang, R., Wang, D., Wang, S., Zhou, J., Chai, Z., Yao, S., Li, J., Lu, L., Liu, Y., et al. (2020). Deliver anti-PD-L1 into brain by p-hydroxybenzoic acid to enhance immunotherapeutic effect for glioblastoma. J. Control Release *320*, 63–72.

Hubkova, B., Velika, B., Birkova, A., Guzy, J., and Marekova, M. (2014). Hydroxybenzoic acids and their derivatives as peroxynitrite scavengers. Free Radic. Biol. Med. *75*, S33–S34.

Ishisaka, A., Ichikawa, S., Sakakibara, H., Piskula, M.K., Nakamura, T., Kato, Y., Ito, M., Miyamoto, K., Tsuji, A., Kawai, Y., et al. (2011). Accumulation of orally administered quercetin in brain tissue and its antioxidative effects in rats. Free Radic. Biol. Med. *51*, 1329–1336.

Itoh, K., Chiba, T., Takahashi, S., Ishii, T., Igarashi, K., Katoh, Y., Oyake, T., Hayashi, N., Satoh, K., Hatayama, I., et al. (1997). An Nrf2/small Maf heterodimer mediates the induction of phase II detoxifying enzyme genes through antioxidant response elements. Biochem. Biophys. Res. Commun. *236*, 313–322.

Kanehisa, M., and Goto, S. (2000). KEGG: Kyoto encyclopedia of genes and genomes. Nucleic Acids Res. *28*, 27–30. https://doi.org/10.1093/nar/28.1.27.

Kelder, T., Pico, A.R., Hanspers, K., van Iersel, M.P., Evelo, C., and Conklin, B.R. (2009). Mining biological pathways using WikiPathways web services. PLoS One *4*, e6447. https://doi.org/10.1371/journal.pone.0006447.

Lev-Vachnish, Y., Cadury, S., Rotter-Maskowitz, A., Feldman, N., Roichman, A., Illouz, T., Varvak, A., Nicola, R., Madar, R., and Okun, E. (2019). L-Lactate promotes adult hippocampal neurogenesis. Front Neurosci. *13*, 403.

Liu, C., Kuei, C., Zhu, J., Yu, J., Zhang, L., Shih, A., Mirzadegan, T., Shelton, J., Sutton, S., Connelly, M.A., et al. (2012). 3,5-Dihydroxybenzoic acid, a specific agonist for hydroxycarboxylic acid 1, inhibits lipolysis in adipocytes. J. Pharmacol. Exp. Ther. *341*, 794–801.

Moon, J.S., Kim, S.H., Oh, S.H., Jeong, Y.W., Kang, J.H., Park, J.C., Son, H.J., Bae, S., Park, B.I., Kim, M.S., et al. (2014). Relaxin augments BMP-2-induced osteoblast differentiation and bone formation. J. Bone Miner Res. *29*, 1586–1596.

Nguyen, T., Nioi, P., and Pickett, C.B. (2009). The Nrf2-antioxidant response element signaling pathway and its activation by oxidative stress. J. Biol. Chem. *284*, 13291–13295.

Nguyen, T., Sherratt, P.J., Nioi, P., Yang, C.S., and Pickett, C.B. (2005). Nrf2 controls constitutive and inducible expression of ARE-driven genes through a dynamic pathway involving nucleocytoplasmic shuttling by Keap1. J. Biol. Chem. *280*, 32485–32492.

Nguyen, T., Sherratt, P.J., and Pickett, C.B. (2003). Regulatory mechanisms controlling gene expression mediated by the antioxidant response element. Annu. Rev. Pharmacol. Toxicol. *43*, 233–260.

Nichols, M., Zhang, J., Polster, B.M., Elustondo, P.A., Thirumaran, A., Pavlov, E.V., and Robertson, G.S. (2015). Synergistic neuroprotection by epicatechin and quercetin: activation of convergent mitochondrial signaling pathways. Neuroscience *308*, 75–94.

Ohno, Y., Oyama, A., Kaneko, H., Egawa, T., Yokoyama, S., Sugiura, T., Ohira, Y., Yoshioka, T., and Goto, K. (2018). Lactate increases myotube diameter via activation of MEK/ERK pathway in C2C12 cells. Acta Physiol. *223*, e13042.

Ortiz-Lopez, L., Marquez-Valadez, B., Gomez-Sanchez, A., Silva-Lucero, M.D., Torres-Perez, M., Tellez-Ballesteros, R.I., Ichwan, M., Meraz-Rios, M.A., Kempermann, G., and Ramirez-Rodriguez, G.B. (2016). Green tea compound epigallo-catechin-3-gallate (EGCG) increases neuronal survival in adult hippocampal neurogenesis in vivo and in vitro. Neuroscience *322*, 208–220.

Pinto, M., Benfeito, S., Fernandes, C., and Borges, F. (2020). Antioxidant therapy, oxidative stress, and blood-brain barrier: the road of dietary antioxidants. In Oxidative Stress and Dietary Antioxidants in Neurological Diseases, V.R.P. Colin and R. Martin, eds. (Academic Press), pp. 125–141.

Plumpe, T., Ehninger, D., Steiner, B., Klempin, F., Jessberger, S., Brandt, M., Romer, B., Rodriguez, G.R., Kronenberg, G., and Kempermann, G. (2006). Variability of doublecortin-associated dendrite maturation in adult hippocampal neurogenesis is independent of the regulation of precursor cell proliferation. BMC Neurosci. *7*, 77.

Prozorovski, T., Schulze-Topphoff, U., Glumm, R., Baumgart, J., Schroter, F., Ninnemann, O., Siegert, E., Bendix, I., Brustle, O., Nitsch, R., et al. (2008). Sirt1 contributes critically to the redox-dependent fate of neural progenitors. Nat. Cell Biol. *10*, 385–394.

Remington, R., Chan, A., Lepore, A., Kotlya, E., and Shea, T.B. (2010). Apple juice improved behavioral but not cognitive symptoms in moderate-to-late stage Alzheimer's disease in an open-label pilot study. Am. J. Alzheimers Dis. Other Demen. *25*, 367–371.

Soni, M.G., Carabin, I.G., and Burdock, G.A. (2005). Safety assessment of esters of p-hydroxybenzoic acid (parabens). Food Chem. Toxicol. *43*, 985–1015.

Spencer, J.P.E. (2009). The impact of flavonoids on memory: physiological and molecular considerations. Chem. Soc. Rev. *38*, 1152–1161.

Tchantchou, F., Chan, A., Kifle, L., Ortiz, D., and Shea, T.B. (2005). Apple juice concentrate prevents oxidative damage and impaired maze performance in aged mice. J. Alzheimers Dis. *8*, 283–287.

Torres-Perez, M., Tellez-Ballesteros, R.I., Ortiz-Lopez, L., Ichwan, M., Vega-Rivera, N.M., Castro-Garcia, M., Gomez-Sanchez, A., Kempermann, G., and Ramirez-Rodriguez, G.B. (2015). Resveratrol enhances neuroplastic changes, including hippocampal neurogenesis, and memory in Balb/C Mice at six months of age. PLoS One *10*, e0145687.

van der Made, S.M., Plat, J., and Mensink, R.P. (2015). Resveratrol does not influence metabolic risk markers related to cardiovascular

health in overweight and slightly obese subjects: a randomized, placebo-controlled crossover trial. PLoS One *10*, e0118393.

Viggiano, A., Viggiano, A., Monda, M., Turco, I., Incarnato, L., Vinno, V., Viggiano, E., Baccari, M.E., and De Luca, B. (2006). Annurca apple-rich diet restores long-term potentiation and induces behavioral modifications in aged rats. Exp. Neurol. *199*, 354–361.

Walker, T.L., and Kempermann, G. (2014). One mouse, two cultures: isolation and culture of adult neural stem cells from the two neurogenic zones of individual mice. J. Vis. Exp. *25*, e51225.

Wang, J., Cui, Y., Yu, Z., Wang, W., Cheng, X., Ji, W., Guo, S., Zhou, Q., Wu, N., Chen, Y., et al. (2019). Brain endothelial cells maintain lactate homeostasis and control adult hippocampal neurogenesis. Cell Stem Cell *25*, 754–767.

Yoo, K.Y., Choi, J.H., Hwang, I.K., Lee, C.H., Lee, S.O., Han, S.M., Shin, H.C., Kang, I.J., and Won, M.H. (2010). (-)-Epigallocatechin-3-gallate increases cell proliferation and neuroblasts in the subgranular zone of the dentate gyrus in adult mice. Phytother. Res. *24*, 1065–1070.

Stem Cell Reports, Volume *16*

Supplemental Information

Apple Peel and Flesh Contain Pro-neurogenic Compounds

Muhammad Ichwan, Tara L. Walker, Zeina Nicola, Jutta Ludwig-Müller, Christoph Böttcher, Rupert W. Overall, Vijay S. Adusumilli, Merve Bulut, Alex M. Sykes, Norbert Hübner, Gerardo Ramirez-Rodriguez, Leonardo Ortiz-López, Enrique A. Lugo-Hernández, and Gerd Kempermann

Supplementary Data

Supplementary Table 1. List of the top 10 upregulated and downregulated genes in quercetin-treated adherent neural precursor cells cultured under differentiation conditions.

Gene ID	Gene symbol	Gene name	Relative expression	Adjusted *p* value
14859	Gsta3	glutathione S-transferase, alpha 3	4.56	0.001
228775	Trib3	tribbles homolog 3 (Drosophila)	3.8	0.002
76650	Srxn1	sulfiredoxin 1 homolog (S. cerevisiae)	3.6	0.001
71839	Osgin1	oxidative stress induced growth inhibitor 1	3.56	0.001
15220	Foxq1	forkhead box Q1	3.38	0.001
23886	Gdf15	growth differentiation factor 15	3.36	0.004
19773	Rln1	relaxin 1	3.2	0.002
14630	Gclm	glutamate-cysteine ligase, modifier subunit	3.14	0.001
53945	Slc40a1	solute carrier family 40 (iron-regulated transporter), member 1	3.1	0.001
12705	Cited1	Cbp/p300-interacting transactivator with Glu/Asp-rich carboxy-terminal domain 1	3.07	0.001
64075	Smoc1	SPARC related modular calcium binding 1	-3.81	0.005
16979	Lrrn1	leucine rich repeat protein 1, neuronal	-2.89	0.003
330166	Miat	myocardial infarction associated transcript (non-protein coding)	-2.84	0.002
70433	Draxin	dorsal inhibitory axon guidance protein	-2.78	0.002
18761	Prkcq	protein kinase C, theta	-2.77	0.002
12799	Cnp	2',3'-cyclic nucleotide 3' phosphodiesterase	-2.75	0.004
18377	Omg	oligodendrocyte myelin glycoprotein	-2.68	0.002
70784	Rasl12	RAS-like, family 12	-2.58	0.002
18481	Pak3	p21 protein (Cdc42/Rac)-activated kinase 3	-2.55	0.002
101488	Slco2b1	solute carrier organic anion transporter family, member 2b1	-2.47	0.001

Supplementary Table 2. List of the differential expression of JNKs and related pro-apoptotic genes in the MAPK pathway in quercetin-treated adherent neural precursor cells cultured under differentiation conditions.

Gene ID	Gene symbol	Gene name	Relative expression	Adjusted *p* value
26420	Mapk9	mitogen activated protein kinase-9 (JNK2)	0.49	0.04
26414	Mapk10	mitogen activated protein kinase-10 (JNK3)	0.95	0.01
12028	Bax	BCL2-associated X protein	0.9	0.01
170770	PUMA	BCL2 binding component 3 (Bbc3)	0.53	0.01
12122	Bid	BH3 interacting domain death agonist	1.05	0.002
26419	Mapk8	mitogen activated protein kinase-8 (JNK1)	-0.57	0.02

Supplementary Table 3. A list of the differentially expressed genes mapped to the PI3 kinase-Akt pathway (KEGG pathways mmu04151) in quercetin-treated adherent neural precursor cells cultured under differentiation conditions.

Gene ID	Gene symbol	Gene name	Relative expression	Adjusted *p* value
22339	Vegfa	vascular endothelial growth factor A	2.17	0.002
20393	Sgk1	serum/glucocorticoid regulated kinase 1	1.87	0.002
13685	Eif4ebp1	eukaryotic translation initiation factor 4E binding protein 1	1.48	0.008
14164	Fgf1	fibroblast growth factor 1	1.47	0.005
11911	Atf4	activating transcription factor 4	1.41	0.013
108079	Prkaa2	protein kinase, AMP-activated, alpha 2 catalytic subunit	1.41	0.012
17246	Mdm2	transformed mouse 3T3 cell double minute 2	1.3	0.005
14696	Gnb4	guanine nucleotide binding protein (G protein), beta 4	1.26	0.004
16590	Kit	kit oncogene	1.23	0.016
12048	Bcl2l1	BCL2-like 1	1.11	0.004
12575	Cdkn1	cyclin-dependent kinase inhibitor 1A (P21)	1.02	0.025
241226	Itga8	integrin alpha 8	0.98	0.011
14268	Fn1	fibronectin 1	0.96	0.025
16410	Itgav	integrin alpha V	0.92	0.01
22628	Ywhag	tyrosine 3-monooxygenase/tryptophan 5 monooxygenase activation protein, gamma polypeptide	0.91	0.024
21898	Tlr4	toll-like receptor 4	0.9	0.005
22341	Vegfc	vascular endothelial growth factor C	0.9	0.012

74769	Pik3cb	phosphatidylinositol 3-kinase, catalytic, beta polypeptide	0.88	0.017
12444	Ccnd2	cyclin D2	0.88	0.024
20181	Rxra	retinoid X receptor alpha	0.87	0.004
18750	Prkca	protein kinase C, alpha	0.86	0.01
14083	Ptk2	PTK2 protein tyrosine kinase 2	0.84	0.004
13640	Efna5	ephrin A5	0.84	0.017
208647	Creb3l2	cAMP responsive element binding protein 3-like 2	0.84	0.02
104099	Itga9	integrin alpha 9	0.8	0.017
12443	Ccnd1	cyclin D1	0.77	0.031
192897	Itgb4	integrin beta 4	0.75	0.002
14205	Figf	c-fos induced growth factor	0.75	0.017
26427	Creb3l1	cAMP responsive element binding protein 3-like 1	0.72	0.003
109333	Pkn2	protein kinase N2	0.71	0.002
226849	Ppp2r5a	protein phosphatase 2, regulatory subunit B (B56), alpha isoform	0.7	0.013
16337	Insr	insulin receptor	0.68	0.03
16194	Il6ra	interleukin 6 receptor, alpha	0.65	0.036
15461	Hras	Harvey rat sarcoma virus oncogene 1	0.63	0.036
18607	Pdpk1	3-phosphoinositide dependent protein kinase 1	0.63	0.012
12977	Csf1	colony stimulating factor 1(macrophage)	0.6	0.02
23797	Akt3	thymoma viral proto-oncogene 3	0.6	0.004
14183	Fgfr2	fibroblast growth factor receptor 2	0.56	0.012
12913	Creb3	cAMP responsive element binding protein 3	0.55	0.009
14182	Fgfr1	fibroblast growth factor receptor 1	0.51	0.03
12831	Col5a1	collagen, type V, alpha 1	0.5	0.008
16402	Itga5	integrin alpha 5 (fibronectin receptor alpha)	0.5	0.029

14706	Gng4	guanine nucleotide binding protein (G protein) gamma 4	0.49	0.002
269643	Ppp2r2c	protein phosphatase 2 (formerly 2A), regulatory subunit B (PR 52), gamma isoform	0.48	0.026
16151	Ikbkg	inhibitor of kappaB kinase gamma	0.43	0.015
19053	Ppp2cb	protein phosphatase 2 (formerly 2A), catalytic subunit, beta isoform	0.43	0.017
19211	Pten	phosphatase and tensin homolog	0.38	0.034
54635	Pdgfc	platelet-derived growth factor, C polypeptide	0.38	0.036
19052	Ppp2ca	protein phosphatase 2 (formerly 2A), catalytic subunit, alpha isoform	0.37	0.014
14936	Gys1	glycogen synthase 1, muscle	0.36	0.044
14745	Lpar1	lysophosphatidic acid receptor 1	0.33	0.026
14171	Fgf17	fibroblast growth factor 17	0.3	0.02
14600	Ghr	growth hormone receptor	0.19	0.018
52432	Ppp2r2d	protein phosphatase 2, regulatory subunit B, delta isoform	0.18	0.026
14377	G6pc	glucose-6-phosphatase, catalytic	0.13	0.04
14170	Fgf15	fibroblast growth factor 15	-0.13	0.032
12189	Brca1	breast cancer 1	-0.27	0.016
72508	Rps6kb1	ribosomal protein S6 kinase, polypeptide 1	-0.34	0.041
78134	Lpar4	lysophosphatidic acid receptor 4	-0.35	0.041
22370	Vtn	vitronectin	-0.37	0.006
12445	Ccnd3	cyclin D3	-0.42	0.02
21827	Thbs3	thrombospondin 3	-0.48	0.036
22059	Trp53	transformation related protein 53	-0.50	0.014
16398	Itga2	integrin alpha 2	-0.52	0.031
13684	Eif4e	eukaryotic translation initiation factor 4E	-0.56	0.022

12830	Col4a5	collagen, type IV, alpha 5	-0.66	0.006
12447	Ccne1	cyclin E1	-0.69	0.047
12832	Col5a2	collagen, type V, alpha 2	-0.69	0.012
56716	Mlst8	MTOR associated protein, LST8 homolog (*S. cerevisiae*)	-0.71	0.013
373864	Col27a1	collagen, type XXVII, alpha 1	-0.71	0.029
12125	Bcl2l11	BCL2-like 11 (apoptosis facilitator)	-0.72	0.005
13649	Egfr	epidermal growth factor receptor	-0.72	0.045
17311	Kitl	kit ligand	-0.79	0.025
12566	Cdk2	cyclin-dependent kinase 2	-0.84	0.023
18709	Pik3r2	phosphatidylinositol 3-kinase, regulatory subunit, polypeptide 2 (p85 beta)	-0.84	0.009
12675	Chuk	conserved helix-loop-helix ubiquitous kinase	-0.9	0.006
21826	Thbs2	thrombospondin 2	-0.95	0.004
12567	Cdk4	cyclin-dependent kinase 4	-0.97	0.005
14168	Fgf13	fibroblast growth factor 13	-1.39	0.014
18595	Pdgfra	platelet derived growth factor receptor, alpha polypeptide	-1.43	0.008
18710	Pik3r3	phosphatidylinositol 3 kinase, regulatory subunit, polypeptide 3 (p55)	-1.45	0.003
14708	Gng7	guanine nucleotide binding protein (G protein), gamma 7	-1.49	0.002

Supplementary Table 4. A list of the differentially expressed genes mapped to the Nrf2-Keap1 pathway (Wikipathways WP1245) in quercetin-treated adherent neural precursor cells cultured under differentiation conditions.

Gene ID	Gene symbol	Gene name	Relative expression	Adjusted *p* value
14859	Gsta3	glutathione S-transferase, alpha 3	4.56	0.001
12608	Cebpb	CCAAT/enhancer binding protein (C/EBP), beta	1.96	0.004
15368	Hmox1	heme oxygenase (decycling) 1	2.24	0.003
17132	Maf	avian musculoaponeurotic fibrosarcoma (v-maf) AS42 oncogene homolog	0.36	0.033
18104	Nqo1	NAD(P)H dehydrogenase, quinone 1	1.91	0.002
18750	Prkca	protein kinase C, alpha	0.86	0.01
14630	Gclm	glutamate-cysteine ligase, modifier subunit	3.14	0.001
50868	Keap1	kelch-like ECH-associated protein 1	0.53	0.01
14629	Gclc	glutamate-cysteine ligase, catalytic subunit	0.87	0.006
18024	Nfe2l2	nuclear factor, erythroid derived 2, like 2	0.34	0.03
26419	Mapk8	mitogen-activated protein kinase 8	-0.57	0.021

Supplementary Table 5. The total flavonoid content in different apple varieties.

Cultivar	Total flavonoid content (equivalent to mg quercetin / 100 g fresh weight)	
	Peel	**Flesh**
Pinova	379 ± 93.95	42.45 ± 17.63
Elstar	428.9 ± 103.7	96.74 ± 32.61
Pilot	344.3 ± 74.19	67.36 ± 25.43
Rebella	186.6 ± 44.4	48.82 ± 15.10
Roter Berlepsch	148.1 ± 60.55	18.74 ± 7.86
Jonagold	87.85 ± 28.45	36.98 ± 15.53

Supplementary Table 6. Peak annotation of UPLC / PDA / ESI-QTOFMS analysis of fraction IV based on accurate mass measurement and high-resolution CID mass spectra.

Peak number	*m/z*, ESI($^+$)	*m/z*, ESI($^-$)	Elemental composition	Comments
1	347.0942, $[M^+Na]^+$	323.0979, $[M^-H]^-$	$C_{12}H_{20}O_{10}$	hexoside
2	339.0668, $[M^+Na]^+$	315.0713, $[M^-H]^-$	$C_{13}H_{16}O_9$	dihydroxybenzoate O-hexoside
3	361.1099, $[M^+Na]^+$	337.1133, $[M^-H]^-$	$C_{13}H_{22}O_{10}$	hexoside, homolog of 1
4	471.1082, $[M^+Na]^+$	447.1132, $[M^-H]^-$	$C_{18}H_{24}O_{13}$	dihydroxybenzoate *O*-(hexoside-pentoside)
5	361.1091, $[M^+Na]^+$	337.1140, $[M^-H]^-$	$C_{13}H_{22}O_{10}$	hexoside, Isomer of 3
6	660.1686, $[M^+H]^+$	658.1546, $[M^-H]^-$	?	?

Supplementary Table 7. List of antibodies

Antibody	Dilution	Supplier	Catalogue #
Primary antibodies			
Goat anti Doublecortin	1:250	Santa Cruz Biotechnology	sc-8067
Mouse anti Idu/BrdU	1:500	BD Bioscience	347580
Mouse anti Map2(ab)	1:1000	Sigma	M-1406
Mouse anti Nestin	1:400	BD Bioscience	611658
Mouse anti S100β	1:1000	Sigma	S 2532
Mouse anti β-Actin	1:1000	Santa Cruz Biotechnology	sc-81178
Mouse anti β-III-Tubulin	1:1000	Promega	G712A
Rabbit anti Vinculin	1:1000	ThermoFisher Scientific	700062
Rabbit anti Cdk4	1:1000	Abcam	ab7955
Rabbit anti HCAR-1	1:100	Sigma	SAB1300090
Rabbit anti cleaved Caspase-3	1:1000	Cell Signaling Technology	9661
Rabbit anti Cyclin D1	1:1000	Abcam	ab16663
Rabbit anti FOX3/NeuN	1:500	Abcam	ab104225
Rabbit anti GFAP	1:2000	Dako	Z0334
Rabbit anti GSTA3	1:1000	Proteintech	16703-1-AP
Rabbit anti Ki67p (NCL)	1:500	Novocastra	NCL-Ki67p
Rabbit anti p27 (C-19)	1:1000	Santa Cruz Biotechnology	sc-528
Rabbit anti phospho-Akt	1:2000	Cell Signaling Technology	4060S
Rabbit anti SOX2	1:500	Merck Millipore	AB5603
Rabbit anti-BCL2L1	1:400	Sigma	AV30475
Rat anti-BrdU	1:500	AbD Serotec	OBT0030
Secondary antibodies			
Donkey anti goat Biotin	1:500	Jackson ImmunoResearch	705-065-147
Donkey anti goat HRP	1:500	Jackson ImmunoResearch	705-035-003
Donkey anti mouse Cy3	1:500	Jackson ImmunoResearch	715-505-151
Donkey anti mouse Cy5	1:500	Jackson ImmunoResearch	715-175-151
Donkey anti mouse DyLight 488	1:500	Jackson ImmunoResearch	715-485-150
Donkey anti rabbit Biotin	1:500	Jackson ImmunoResearch	711-065-152
Donkey anti rabbit Cy3	1:500	Jackson ImmunoResearch	711-165-152
Donkey anti rat Biotin	1:500	Jackson ImmunoResearch	712-065-153
Donkey anti rat Cy 3	1:500	Jackson ImmunoResearch	712-225-153
Goat anti mouse HRP	1:500	Jackson ImmunoResearch	115-035-003
Goat anti rabbit horseradish peroxidase (HRP)	1:500	Jackson ImmunoResearch	111-035-003
Goat anti rat HRP	1:500	Jackson ImmunoResearch	112-035-003

Supplementary Table 8. Primer sequences

Primer name	Sequence (5'-3')
Bcl2l1 Forward	GCGTGGAAAGCGTAGACAAG
Bcl2l1 Reverse	GCTGCATTGTTCCCGTAGAG
Bcl2l11 Forward	GCCAGGCCTTCAACCACTAT
Bcl2l11 Reverse	GCTCCTGTGCAATCCGTATC
β-actin Forward	TGACCCAGATCATGTTTGAGA
β-actin Reverse	GGAGAGCATAGCCCTCGTA

Supplemental Experimental Procedures

Apple fractionation

The first fractionation steps were performed using the solvent fractionation method. The extracts were dissolved in ddH_2O and 1 volume of ethyl acetate was added. Using a separation funnel, the water and ethyl acetate phase was separated and collected. The solvent was evaporated, and the water fraction was further separated in the mixture of water and butanol (1:1). From these steps, 3 fractions were obtained each from apple peel and the solvent in all fractions was evaporated until maximum dryness. The active water fraction from the butanol separation was further fractionated by column separation using a Reverse phase C8 column (Vydac). The fraction was dissolved in 20% methanol solution before being injected into the column and then eluted with 20%-, 40%-, 60%- and 100% methanol consecutively for 30 minutes each. The elutes were then dried using centrifugal evaporator prior to being tested in the neurosphere assay. The active fraction (the one collected in 40% methanol) was further fractionated using Eurosphere C18 column using a gradient system with 1% aqueous acetic acid and 100 % acetonitrile (ACN) as the solvent. The gradient started with 80% ACN, then after 20 minutes decreased to 50% ACN, further decreased to 30% ACN within 20 minutes and finally within 20 minutes to 5%, followed by an equilibration step to the initial run condition. In this separation technique, 4 fractions were collected from different time ranges, i.e. minute 0-10, 10-20, 20-30 and 30-60, respectively. The solvent was evaporated in centrifugal evaporator prior to the neurosphere assay. The active fraction from this step was then analyzed using UPLC-MS system for structure elucidation.

Compound elucidation by UPLC/ESI-QTOFMS

Chromatographic separations were performed at 40°C on an Acquity UPLC system (Waters) equipped with a HSS T3 column (100 Å~ 1.0 mm, particle size 1.8 µm, Waters) applying the

following binary gradient at a flow rate of 150 µl min-1: 0-1 min, isocratic 95% A (water/formic acid, 99.9/0.1 v/v), 5% B (acetonitrile/formic acid, 99.9/0.1 v/v); 1-16 min, linear from 5 to 50% B; 16-18 min, isocratic 95% B; 18-20 min, isocratic 5% B. The injection volume was 2.6 µl (full loop injection). Eluting compounds were detected from 190-500 nm using a photodiode array detector (Waters) and from m/z 100-1000 using a MicrOTOF-Q hybrid quadrupole time-of-flight mass spectrometer (Bruker Daltonics) equipped with an Apollo II electrospray ion source in negative ion mode. The following instrument settings were applied: nebulizer gas, nitrogen, 1.6 bar; dry gas, nitrogen, 6 l/min, 190°C; capillary, +4000 V; end plate offset, -500 V; funnel 1 RF, 200 V; funnel 2 RF, 200 V; in-source CID energy, 0 V; hexapole RF, 100 V; quadrupole ion energy, 3 eV; collision gas, argon; collision energy, 10 eV; collision RF 200/400 V (timing 50/50); transfer time, 70 µs; pre pulse storage, 5 µs; pulsar frequency, 10 kHz; spectra rate, 3Hz. Mass spectra were acquired in centroid mode. Calibration of m/z was performed for individual raw data files on lithium formate cluster ions obtained by automatic infusion of 20 µl lithium hydroxide (10 mM) in the mixture of isopropanol/water/formic acid, 49.9/49.9/0.2 (v/v/v) respectively at the end of the gradient using a diverter valve. For the acquisition of collision-induced dissociation mass spectra, appropriate precursor ions were isolated using the first quadrupole (isolation width m/z 4) and fragmented inside the collision cell applying collision energies in the range of 15-30eV.

Total flavonoid assay

Total flavonoids in apple cultivars were measured using the sodium borohydride/chloranil-based assay as described previously (He and Liu, 2008). Dried samples and quercetin standards were reconstituted in 1 ml THF/EtOH (1:1,v/v) in a glass test tube. 0.5 ml of 50 mM NaBH4 and 0.5 ml of 74.56 mM AlCl3 solution, were added to each tube followed by a 30 min mixing step at RT. An additional 0.5 ml of NaBH4 solution was added with continuing shaking for a further 30 min at

RT. Subsequently, 2 ml of 0.8 M of cold acetic acid solution was added, thoroughly mixed and then incubated in the dark for 15 min. The tubes were then heated to 100ºC with shaking for 60 min after adding 1ml of 20 mM chloranil. The tubes were cooled and the final volume was brought to 4 ml with methanol. Then, 1 ml of 1052 mM vanillin was added into each tube and mixed thoroughly. Finally, 2 ml of concentrated HCl was added into each tube and kept in the dark for 15 min after a thorough mix. For detection, 200 µl of final reaction solution was added into each well of a 96-well plate and the absorbances were measured using a microplate reader at 490 nm.

Immunostaining

In vitro immunostaining

The fixed cells were washed twice with 0.9% NaCl and then incubated in 1N HCl at 37°C for 30 min, followed by one wash with 0.1M borate buffer, pH 8, and two washes with PBS. The blocking step was performed in 10% donkey serum and 0.2% Triton X-100 in PBS at RT for 1 h. Anti-BrdU antibody (1:500) in antibody solution (3 % donkey serum and 0.1 % Triton X-100) was subsequently dispensed on each coverslip and incubated either for 2 h at RT or overnight at 4°C. After three washes with PBS, the cells were incubated with fluorescence secondary antibody (1:500, in 3 % donkey serum and 0.1 % Triton X-100) for 90 min at RT. Following two washes with PBS cells were incubated for 10 min with Hoechst 33342 (1:3000 in PBS). After a final two washes with PBS, the coverslips were mounted on glass slides using Aqua-Poly/Mount for fluorescence microscopy. Cell counting was performed using a Leica DM5500B fluorescence microscope with StereoInvestigator software. The number of $BrdU^+$ cells in a given population of cells was quantified from several visual fields and the average was presented as the cell percentage. For all other fluorescence staining the above protocol was followed but omitting the HCl step. For HCAR-1 staining, 0.2% Triton X-100 was replaced with 0.2 % saponin.

Fluorescence and DAB immunostaining on brain tissue

A one-in-six series of sections was blocked in blocking solution for 1 h at RT prior to overnight incubation with primary antibodies at 4ºC. After a washing step with PBS, incubation with fluorescence secondary antibody was done for 3-4 h at RT. The tissues were subsequently mounted on glass coverslips with Aqua Polymount. For 3,3'-diaminobenzidine (DAB) staining, the sections were initially incubated with 0.6% H_2O_2 for 30 min. After washing with TBS, sections were incubated with 1 h blocking solution followed by overnight incubation with primary antibodies. The sections were incubated with biotinylated secondary antibodies for 4 h at RT followed by incubation with avidin/biotinylated enzyme complex solution (ABC elite) for 1 h at RT. Thorough washing steps were performed between incubation steps. The chromogen DAB was used as the enzyme substrate. The sections were mounted on gelatin-coated glass slide, dehydrated in Neoclear® solution and then covered with a glass coverslip in Neo-mount® solution. Images were acquired using a Plan-Apochromat 20x/0.8 air objective on the LSM 780.

Cell quantification in brain sections (BrdU-, CldU-, DCX- or IdU-labeled cells)

The number of labeled cells was determined in series of every sixth section. Positive cells were counted throughout the rostro-caudal axis of the granule cell layer using 40x objectives. The resulting numbers were multiplied by six to estimate the total number of labeled cells. For phenotyping, the level of colocalization between $NeuN^+$ or $S100\beta^+$ cells was determined in 100 randomly selected cells for each dentate gyrus and displayed as a percentage.